Chapter 6

Lowering Energy Spending Together With Compression, Storage, and Transportation Costs for Hydrogen Distribution in the Early Market

Didier Grouset* **and Cyrille Ridart†**

Université de Toulouse, IMT Mines Albi, UMR CNRS 5302, Centre RAPSODEE, Campus Jarlard, Albi, France, †HERA—ALBHYON, Technopole Innoprod, rue Pierre Gilles de Gennes, Albi, France

6.1 INTRODUCTION

6.1.1 Hydrogen Supply Chain and Energy Requirements

Future developments in hydrogen fuel cell vehicles promise an important ***decrease in the final spent energy*** and in greenhouse gas and pollutant emissions from transportation. This is mainly due to the qualities of hydrogen fuel cells: high efficiency for chemical to electric conversion, no other product than water, no pollutant emission, and no noise. Nevertheless, to quantify the benefits of hydrogen as a new energy carrier, the ***overall energy chain*** has to be considered, from the primary energy used for hydrogen production to the final step of the useful energy spent for the vehicle movement. Indeed, great care has to be taken so that the decrease in the final spent energy does not induce too large an increase in the energy spent in the intermediate steps of hydrogen ***production, compression, storage, transportation***, and ***distribution***.

Nowadays, everybody would agree that the primary energy for the future large-scale ***production*** of hydrogen energy has to be renewable, through electrolysis of renewable electricity (photovoltaic, wind, hydraulic, etc.), through reforming of renewable hydrocarbons (e.g., biogas), through biomass gasification, and possibly others.

An advantage of hydrogen is that sources for its production are numerous and widespread over the world, so that its production is possible nearly everywhere and close to its valorization location. ***Transportation*** can then be avoided

Hydrogen Supply Chain. https://doi.org/10.1016/B978-0-12-811197-0.00006-3

or reduced to short distances and the costs and energy spending can be saved for hydrogen energy. This is not the case for fossil fuels, which will have to be transported over longer and longer distances of up to several thousand kilometers between their production sites and their distribution sites, resulting in losses of energy and CO_2 emissions; for example, a loss of about 20% of the energy content of natural gas for its pipeline transportation over 5000 km! Currently, with few hydrogen production sites and truck transportation over distances of several hundred kilometers, similar energy spending and CO_2 emissions can be encountered with industrial hydrogen or with hydrogen for energy in the very early market; but solutions under development will eliminate this problem, as shown in this chapter.

Compression of hydrogen for its storage has also to be considered with care; indeed, it is a highly energy consuming operation, as pointed out by Klell et al (2007). Hydrogen is a very light and bulky gas and its compression requires a lot of energy as the green curve in Fig. 6.1 shows. The isothermal compression work from 0.1 to 100 MPa represents >7% of the hydrogen energy content (7.2% of LHV_{H2}, hydrogen low heating value, which is 120 MJ/kg). One should keep in mind that this only represents the mechanical energy transferred to hydrogen in the ideal isothermal compression and that efficiency losses have to be added; any warming of hydrogen during compression, friction in the compressor, or inefficiency of the electric motor will increase the spent energy. Moreover, the efficiency for electric energy production from chemical energy should also be considered (50% in the best cases). Thus, if not processed with care, the compression step could be responsible for more than a 20% loss of the

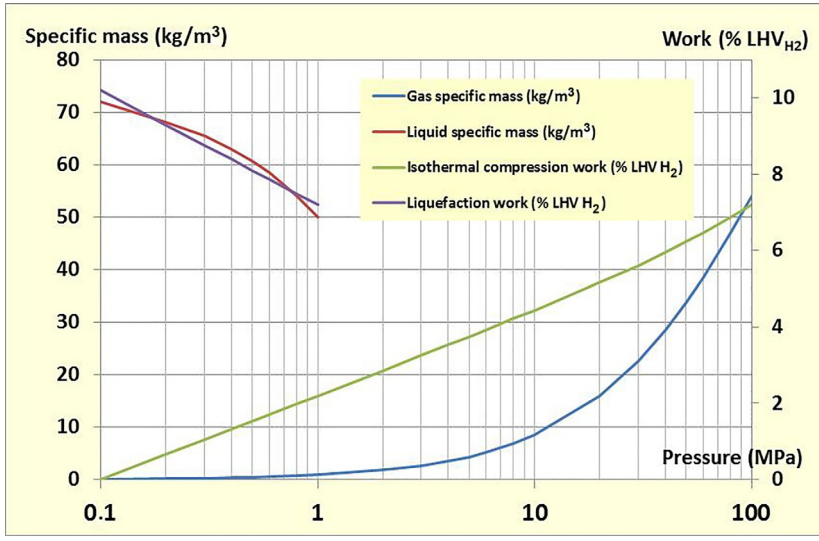

FIG. 6.1 Specific mass and minimum work for compression and liquefaction of hydrogen as a function of pressure, as in Klell et al. (2007).

hydrogen electric energy potential. However, compressing hydrogen to >70 MPa is a necessity to refill vehicle tanks at that pressure! On the other hand, using liquid hydrogen would not be a better solution, as the violet curve of the same figure shows even higher energy needs for the liquefaction of hydrogen. Hopefully, as shown in this chapter, some good practices can lower this energy spend.

The different steps of hydrogen production, compression, and transportation are linked together by the ***storage***, for which different technologies are now matured. Only high-pressure gaseous storage is considered here. Steel bottles or tubes (type 1 vessels) have been used for a very long time and are now challenged in cost, especially for very high pressure, by composite material bottles with an aluminum or plastic internal liner (type 3 or 4 vessels). This study quantifies the savings induced by the light weight of these storage bottles.

Finally, concerning the ***distribution***, many studies have been conducted during the last two decades concerning the most secure way to fill hydrogen car tanks. Some of them have been carried out by international teams that included researchers from different car companies, gas companies, hydrogen technology companies, and research centers, and have been reported, for example, at successive NHA (National Hydrogen Association) congresses, as in Schneider et al. (2005) or Maus et al. (2008). They resulted in the release in July 2014 of a last version of the SAE-J6201 standard (SAE International, 2014) for fueling protocols for gaseous hydrogen vehicles under 35 or 70 MPa pressures, on which are based all current and future refueling stations.

The contribution of compression and storage to the investment cost of a hydrogen refueling station (HRS) is known to be high; following Mintz et al. (2009), it is one-half to two-thirds the cost, according to the HRS size. Thus, it seems important to focus on these costs to understand how they contribute to the overall cost of the delivered hydrogen.

6.1.2 Refueling Principles: Current Practices

In the current practice for rapid filling (Parks et al., 2014; Rothuizen and Rokni, 2014), the vehicle tanks are filled at their nominal pressure simply by pouring available hydrogen from a cascade of buffers, as shown in Fig. 6.2. These buffers have been previously filled with hydrogen at a higher pressure by a compressor connected to the hydrogen production unit, or to a mass intermediate storage. A regulation valve controls the mass flow rate delivered to the tank and the pressure rise in the tank, according to the SAE-J2601 standard (SAE International, 2014).

The performance metrics of an HRS are: delivering pressure, time for filling a tank, and delivering capacity at the peak hour.

- Delivering pressure: two standards, 35 and 70 MPa, coexist for hydrogen vehicle tank pressure.

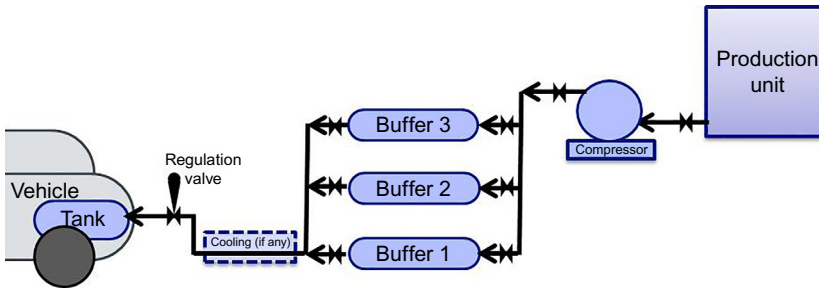

FIG. 6.2 Schematic view of the equipment used for filling hydrogen vehicle HP tanks.

- Time for refueling: the pressure difference between the very high pressure of the buffer storage (e.g., 45 or 90 MPa) and the tank ensures rapid filling. A cooling of the hydrogen is sometimes implemented: it is recommended by SAE-J2601 to allow filling within 3 min in nearly all conditions of ambient temperature and initial tank pressure. Small hydrogen refueling stations do not refrigerate hydrogen and cannot guarantee 3 min refueling.
- The peak hour performance relies mainly on the mass of hydrogen stored in the HP buffers and only incidentally on the mass flow rate of the compressor. In fact, this results from a cost optimization; compressors are expensive and it is cheaper to have a small compressor working nearly all day long to fill buffers than a large compressor with the possibility to fill the tank directly within a few minutes.

Bulk storage at an intermediate pressure is considered as a basic feature of an HRS when connected to a hydrogen pipeline (a 17.2 MPa bulk storage is considered in Parks et al. (2014)), when supplied by trucked trailers (Reddi et al., 2014), or with onsite production (between 20 and 35 MPa in Rothuizen and Rokni (2014)).

The HP buffer storage is usually made of several vessels that can be isolated and connected successively to the vehicle tank. They are always connected to the tank in the same order. The compressor fills the buffers from the bulk storage with a priority for the highest-pressure buffer (number 3 in Fig. 6.2), so that the buffers finally form a pressure cascade, from 35 to 90 MPa for a 70 MPa refueling as recommended in Rothuizen and Rokni (2014).

6.1.3 Content and Objectives

The present chapter is dedicated to the optimization of cost and of energy consumption of compression, transportation, and storage for hydrogen distribution in the current early hydrogen energy market.

Specific emphasis is put on energy needs; whereas costs have often been studied, quantitative information concerning energy consumption are in fact less available. For example, Rothuizen and Rokni (2014) writes as well that

the energy consumption of HRSs are unknown; Wipke et al. (2012) reports variations by a factor of 10 for compression energy consumption; Gardiner (2009) gives more general figures for compression or liquefaction energies.

This chapter aims as well to present the equations necessary to calculate the basic design features of compression, storage, and transportation equipment, and to evaluate cost and energy. Simple models are formulated, together with their simplifying assumptions, so that it becomes possible to transpose the approach to specific cases other than those discussed here.

This chapter is concerned with current or near-future implementations of the emerging market for hydrogen energy, especially in France. So it only considers small HRSs (from 20 to 200 kg/day), whereas most other papers are concerned with long-term perspectives for a developed hydrogen market with large HRSs; 850, 1000, and 1330 kg/day in Parks et al. (2014), 250 kg/day in Reddi et al. (2014). The costs generated here are for current implementations; they were issued from commercial consultations in 2015 and 2016 and no reduction factor has been applied for mass production, which will undoubtedly occur in the next decade, especially for composite pressure bottles, but also for compressors.

First, in Sections 6.2 and 6.3, general technical and economic data concerning compression and storage, the way they were obtained, and how to calculate them, is presented and discussed.

Then two different cases are studied. In Section 6.4, the case of a refueling station on the site of the hydrogen production is analyzed. In this case, the energy spent for the hydrogen distribution is linked to the compressor consumption, to the cooling of the compressor, and, if any, to the cooling of the hydrogen before being delivered to the vehicle tank.

In Section 6.5, the case of a production unit providing hydrogen to several distant refueling stations is considered. The different steps leading to hydrogen distribution are described both in the current practice and when using better practice, evaluating for each the energy consumption, CO_2 emission, investment cost, and operation cost in order to estimate globally for these steps (excluding the production step and the final distribution step), the total cost of ownership (TCO) in €/kg, the specific consumption in kWh/kgH_2, and the specific emission in t_{CO2}/t_{H2}.

6.2 TECHNICAL DATA FOR COMPRESSION AND STORAGE

This section presents the general technical data that will be used in following sections. There will also be a discussion of these data with respect to data used by other authors in similar papers, where appropriate.

6.2.1 Thermodynamic Data for Hydrogen

Hydrogen in not a perfect gas and correct thermodynamic data have to be used in order to get good estimations of heat and work exchanged during heating,

cooling, or compression. More precisely, the evolutions of the specific mass, ρ, the specific internal energy, u, the enthalpy, h, the heat capacity, c_v, c_p, and the entropy, s, with temperature and pressure (p,T), are needed. Different sources can be used for this. Klell et al. (2007) gives interesting information and (T,s) diagrams at low temperature. SAE International (2014) gives, in its appendix, regressions for ρ, u, h, and c_v as functions of (p,T). Lemmon and Leachman (2008) from NIST derived a state equation for hydrogen in which the compressibility factor $Z(p,T)$ is calculated through a 9-term regression, each term needing three coefficients, according to the formula:

$$Z(p,T)=\frac{p}{\rho RT}=1+\sum_{i=1}^{9}a_i\left(\frac{100\,\mathrm{K}}{T}\right)^{b_i}\left(\frac{p}{1\,\mathrm{MPa}}\right)^{c_i} \tag{6.1}$$

The accuracy of this regression is very good; 0.15%, in a large range of p (up to 200 MPa) and T (150–1000 K). Then, knowing $Z(p,T)$ allows a calculation of u and h.

Calculations in this chapter also use hydrogen thermodynamic data available from the chemical data webbook published by NIST Chemical Webbook (n.d.). From the values of $\rho(p,T)$ read in the tables, $Z(p,T)$ can be calculated and polynomial regressions, simpler than Eq. (6.1), have been derived. The NIST webbook also gives the values for u and h, s, c_v,c_p used in this chapter. An example of the result for $Z(p,T)$ variation with p ranging from 0.1 to 90 MPa is given in Fig. 6.3; $Z(p,T)$ increases from 0.99 at ambient pressure to 1.63 at 90 MPa at $T=273$ K.

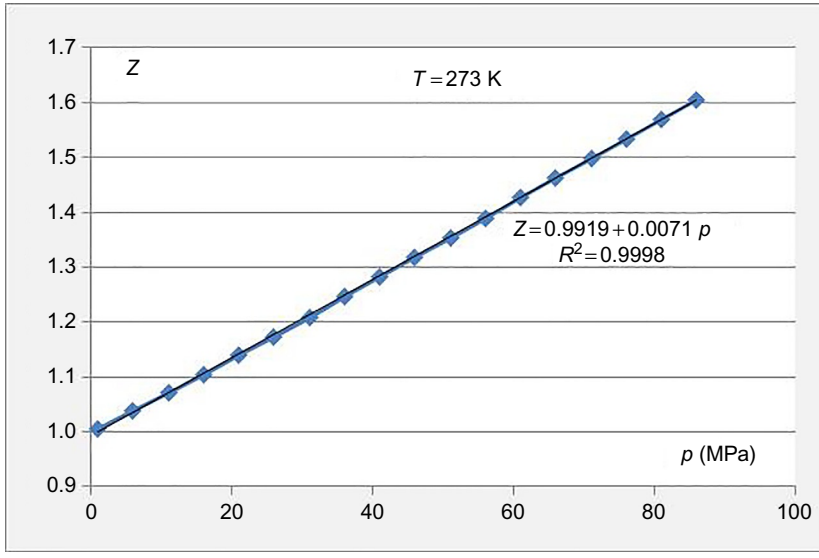

FIG. 6.3 Variation of hydrogen compressibility factor $Z(p,T)$ for $T=273$ K.

6.2.2 Compression Work, Isothermal or Adiabatic

The useful work developed by a compressor is equal to the work of the pressure forces during the volume decrease of the compressed hydrogen. Pressure and volume are linked through the gas state equation, so for a mass m or mole number n, the compression work is:

$$W_{useful} = -\int_{V=V_0}^{V_f} p * dV = -\int_{V=V_0}^{V_f} Z(p,T)\frac{nRT}{V} * dV = -m * {}^{R}\Big/_{M} \int_{V=V_0}^{V_f} Z(p,T) * \frac{T}{V} * dV \tag{6.2}$$

As hydrogen has the lowest molar mass M of all gases, the mass compression work will be the highest. Moreover, hydrogen is a nonperfect gas with $Z_{H2}(p,T) > 1$, which means that the compression work will be higher than for a perfect gas or for methane, which is an imperfect gas with $Z_{CH4}(p,T) < 1$. The high values of $Z(p,T)$ lead to a significant increase of the useful work with respect to a perfect gas.

In the case of an *isothermal* compression of a perfect gas, Eq. (6.2) can easily be integrated and leads to the *useful compression energy*, reference energy as the lowest possible:

$$W_{isothermal,\,perfect} = -m * {}^{R}\Big/_{M} * T_0 \int_{V=V_0}^{V_f} \frac{dV}{V} = m * {}^{R}\Big/_{M} * T_0 * \ln\left({}^{p_f}\Big/_{p_0}\right) \tag{6.3}$$

For hydrogen or any imperfect gas, the integral has to be calculated step by step, but the result can be expressed as:

$$W_{isothermal,\,H2} = \overline{Z_{H2_0}^{f}} * W_{isothermal,\,perfect} \tag{6.4}$$

where the coefficient $\overline{Z_{H2_0}^{f}}$ represents the real gas effect, comprised between $Z_{H2}(p_0,T_0)$ and $Z_{H2}(p_f,T_f)$. The result, divided by the hydrogen LHV, is plotted in Fig. 6.1 as a function of p_f for $p_0 = 1$ bar.

Furthermore, compressing a gas leads to an increase in its temperature, increasing its volume, and so increasing also the compression work. If the compression is *adiabatic*, temperature and pressure are linked, so that the final temperature and the *isentropic* compression work of a perfect gas can be expressed as:

$$W_{isentropic,\,perfect} = m * {}^{R}\Big/_{M} * T_0 * \frac{\gamma}{\gamma - 1} * \left[\left({}^{p_f}\Big/_{p_0}\right)^{\frac{\gamma-1}{\gamma}} - 1\right] \tag{6.5}$$

$$T_f = T_0 * \left({}^{p_f}\Big/_{p_0}\right)^{\frac{\gamma-1}{\gamma}} \tag{6.6}$$

For hydrogen, an imperfect gas, the result can be written as:

$$W_{isentropic,\,H2} = \overline{Z'_{H2_0}^{f}} * W_{isentropic,\,perfect} \tag{6.7}$$

Eqs. (6.3) and (6.5) clearly show that the main parameter is the pressure ratio $r_p = {}^{p_f}/_{p_0}$ and also that the lower the initial temperature, T_0, the lower is the compression work. In the case of large compression ratios, the isentropic temperature increase can be large and the isentropic compression work will be much larger than the isothermal compression work. For example, for a compression from 2 to 45 MPa, the pressure ratio is 22.5 and

$$T_{f,\,isentropic} = T_0 * (22.5)^{\frac{\gamma-1}{\gamma}} = 2.43 * T_0, \quad \text{so}: W_{isentropic,\,perfect} = 1.61 * W_{isothermal,\,perfect}.$$

It is clear that cooling the gas and the compressor is necessary to lower the compression work. Splitting the compression into several successive intercooled stages is also beneficial.

6.2.3 Compression Efficiency

Moreover, friction and efficiency losses also increase the gas temperature and the electric power needed by the compressor. The question is how to estimate compressor efficiency? A lot of parameters influence the efficiency, and first of all is the compressor technology. Several mature technologies can be found for hydrogen compression, such as reciprocating compressors, diaphragm compressors, and pneumatic or hydraulic boosters.

It is not the purpose of this chapter to present details about these safe and mature technologies, but to focus on information concerning the energy needs in compression. The diaphragm compressor will have better energy efficiency, defined as the ratio between the energy transferred to the compressed hydrogen and the consumed electric energy:

- The friction of pistons in the booster cylinders generates higher losses than the deformation of the diaphragm. It can also be understood that friction will be relatively higher for smaller capacity compressors.
- Losses occur in the compression of the working fluid (oil or air) in boosters, and these losses will be more elevated for compressed air than for compressed oil; while the diaphragm compressor crank benefits from a direct electric drive.
- In case of low or medium charge of the compressor (e.g., when the storage pressure is only at 5 or 20 MPa for a nominal pressure of 45 or 90 MPa), the diaphragm compressor will adapt and will need less energy, whereas the booster always consumes the same energy; the oil has been compressed up to 20 MPa (or the air compressed up to 0.8 MPa) and the extra energy will be lost.

It is important to define the way to calculate the efficiency. Nexant Inc. et al. (2008) recommends defining efficiency with respect to isentropic (or adiabatic) work and reports isentropic efficiencies in the range of 86%–92% for large

reciprocating compressors. But the compressors considered for hydrogen distribution in general, and specifically in the present study, are really smaller. Parks et al. (2014), Rothuizen and Rokni (2014), and Reddi et al. (2014) follow this recommendation and use isentropic efficiency. Rothuizen and Rokni (2014) uses a formula from chemical processes (Smith, 2005) for the variation of isentropic efficiency with the pressure ratio and assumes that all efficiency losses contribute to increase hydrogen enthalpy (no external losses), which again is acceptable for large uncooled compressors. Rothuizen and Rokni (2014) and Reddi et al. (2014) use a 65% isentropic efficiency. Parks et al. (2014) underlines the lack of experimental data, and a large dispersion, by a factor of 10, of the few compressor consumption data reported in Wipke et al. (2012) for hydrogen distribution, while in 2013 DOE estimated consumption from 2 to 4 kWh/kgH2 for 35 MPa refueling with an efficiency of about 65% and targets 80% in 2020.

Indeed, efficiency varies greatly with the compressor technology, its capacity, its nominal pressure ratio, and the current pressure ratio. It is also important to consider each single stage, as recommended in Gardiner (2009) and followed in Rothuizen and Rokni (2014), as intercooling considerably reduces the final temperature and isentropic power.

Yet, compressors always exchange heat with the ambient air; for small compressors this can be significant with respect to the necessary heat to cool the compressed hydrogen, while for medium or large capacities, boosters or diaphragm compressor heads are equipped with cooling jackets. Isothermal work is the reference as the lowest needed to compress a gas, and so its calculation relevant. Nevertheless, cooling is never totally efficient, leaving a residual heating of hydrogen during compression. Thus, it seems relevant to calculate the efficiency with respect to both isothermal and isentropic power. In this study, the average of isothermal and isentropic work for each stage is used (Eqs. 6.5 and 6.7). Thus, the electric power needed *for each stage* of a compressor is calculated as follows:

$$P_{eleccomp\,H2} = \frac{1}{h_{comp}}\left(\dot{W}_{isothermal,H2} + \dot{W}_{isentropic,H2}\right)/2 \tag{6.8}$$

Indeed, very large variations in efficiency are found. For small capacity pneumatic boosters, the efficiency can be very low. For example, for compressing 10 kg/day from 5 to 45 MPa an efficiency of 10%–15% has been calculated according to supplier data. Hydraulic boosters are slightly higher, and 15%–20% has been calculated. On the opposite end of the spectrum, for a large 2-stage cooled diaphragm compressor, compressing at its nominal point 850 kg/day from 1.2 to 25 MPa at 27°C and consuming 73.5 kW, an efficiency of 59% has been calculated following Eq. (6.8). With respect to isentropic power only, which is 48 kW with two stages, the isentropic efficiency is 65.2%, which is fully coherent with Parks et al. (2014) and Reddi et al. (2014). Forgetting the two stages and considering only one, would incorrectly lead to an isentropic power of 62 kW and an apparent efficiency of 84.5%.

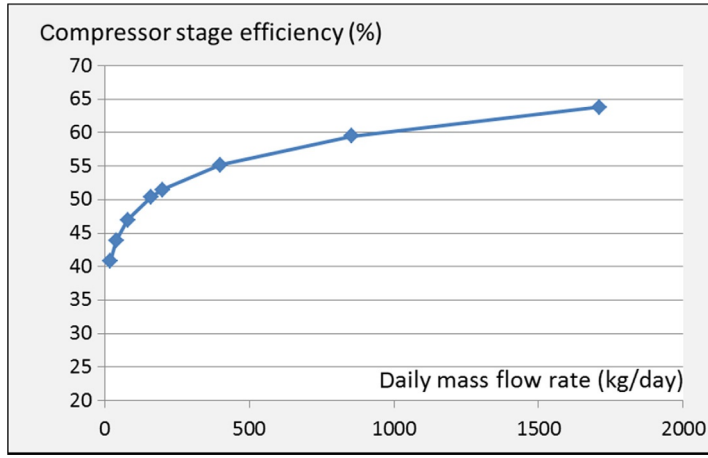

FIG. 6.4 Estimated effect of nominal capacity of a cooled diaphragm compressor on its stage efficiency.

Furthermore, it is known that large compressors have a better efficiency than small ones, and in this study considering cooled diaphragm compressors, while more data from suppliers are needed, the effect of capacity on efficiency will be calculated by a power law according to Eq. (6.9) and presented in Fig. 6.4.

$$h_{comp} = h_{comp,0}\left(\dot{m}/\dot{m}_0\right)^p \quad h_{comp,\,0} = 60\% \quad \dot{m}_0 = 850^{\text{kg}}/_{\text{day}} \quad p = 0.1 \tag{6.9}$$

6.2.4 Cooling Needs

Compressor heads have to be cooled to keep the compression as isothermal as possible; hydrogen has to be cooled at the exit of each compression stage as well. The necessary cooling power can easily be estimated according to the thermodynamic law, which teaches that during a fluid transformation, the enthalpy variation is equal to the sum of the heat and work exchanged with the outside of the system:

$$\Delta H = W + Q \tag{6.10}$$

In the case of a perfect gas, the enthalpy only depends on temperature; as the gas recovers its initial temperature at the end of the compression + cooling process, then:

$$T_f = T_0 \quad \Delta H_{perfect} = 0 \quad \text{and} \quad Q_{cooling} = -W_{comp} \tag{6.11}$$

This equation shows that a heat equivalent to the whole compression work provided to the gas has to be extracted from the system. Moreover, all losses in the compressor, drive, and electric motor convert into heat and also have to be

extracted. Then, it is a cooling power equivalent to the electric power that has to be provided, through exchange with a cooling fluid and through natural convection with the ambient air.

Now, hydrogen is not a perfect gas and the variation of its enthalpy with temperature and pressure can be calculated using data from NIST Chemical Webbook (n.d.). According to Eq. (6.10), the cooling needs will slightly decrease due to the variation of enthalpy with pressure:

$$Q_{cooling,H2} = -W_{comp,H2} + m\left(h_{H2}\left(T_0, p_f\right) - h_{H2}(T_0, p_0)\right) \tag{6.12}$$

Cooling is assumed to be provided through a frigorific machine with a performance coefficient $COP_{cooling}$ of 3 and thus the electrical power of this machine is:

$$P_{eleccoolingH2} = \frac{1}{COP_{cooling}}\left(P_{eleccomp\,H2} - \dot{m}\left(h_{H2}\left(T_0, p_f\right) - h_{H2}(T_0, p_0)\right)\right) \tag{6.13}$$

6.3 ECONOMIC DATA FOR COMPRESSION AND STORAGE

This section presents economic data used in the following sections and discusses them with respect to data from other authors in similar papers, where appropriate.

6.3.1 Compressor Investment Cost

Some spots of information can be found in a number of papers, and especially in Parks et al. (2014), Reddi et al. (2014), and Nexant Inc. et al. (2008) concerning the investment cost of compressors, but few correlations or models are suggested. For example, Reddi et al. (2014) gives a correlation of a parabolic form for the investment cost as a function of capacity (kg/h). Nexant Inc. et al. (2008) recommends a linear increase of price with flow rate, but the range of flow rates is higher than that considered in this paper, mainly above 500 Nm^3/h.

Three compressor manufacturers were queried during 2014 and 2015, covering large ranges for normal flow rate, Q_v, from 5 to 460 Nm^3/h, for inlet pressure, p_0, from 0.7 MPa to 2.5 MPa and for pressure ratios, r_p, from 18 to 64. Quotations were analyzed in order to derive a model for estimating the investment cost of compressors. The size of the cylinders or diaphragms of a compressor depends on the real volume flow rate at the inlet, which is proportional to the normal flow rate, Q_v, divided by the inlet pressure. Indeed, the parameter, Q_v/p_0, appears to be the most relevant and a correlation of the form of Eq. (6.14) has been built:

$$Cost_{comp} = Cost_{comp,0} * a * e * \left\{\left(Q_v/p_0\right)\Big/\left(Q_{v,0}/p_{0,0}\right)\right\}^d \tag{6.14}$$

with $Cost_{comp,0} = 130\text{k\$}, a = 1.04, Q_{v,0} = 40\text{Nm}^3/\text{h}, p_{0,0} = 2\text{MPa}$ and $d = 0.31$.

A shift appeared between manufacturers, represented by the factor e, called the trademark effect, and varied between 0.78 and 1.0 according to the manufacturer. When corrected by this e effect, the costs compare well between two manufacturers, as shown in Fig. 6.5.

It was not possible to find a clear effect of the inlet pressure, nor of the pressure ratio; attempts led to nonrelevant effects and bad correlation coefficients. However, increasing these parameters should have an effect on the design of the compressor, increasing its cost, so a light effect is suggested and introduced in Eq. (6.15):

$$Cost_{comp} = Cost_{comp,0} * a * e * \left\{ \left({}^{Q_v}/_{p_0} \right) / \left({}^{Q_{v,0}}/_{p_{0,0}} \right) \right\}^d * \left({}^{p_0}/_{p_{0,0}} \right)^b * \left({}^{r_p}/_{r_{p,0}} \right)^c \tag{6.15}$$

with $b = 0.1, c = 0.1, r_{p,0} = 22.5$.

- When the correlation from Reddi et al. (2014) is used, the cost obtained for a 3.6 kg/h compressor with an output pressure of 97 MPa would be 172 k$, whereas our correlation gives 145 k$, 15% less, but the quotation seems to date from 2007 in Reddi et al. (2014).
- In Parks et al. (2014) the cost given is also higher. A 35 kg/h 2-stage diaphragm compressor with a 2 MPa inlet pressure and a 45 MPa outlet is 376 k$ (2013), whereas the correlation leads to 280 k$, 26% lower, but Parks et al. (2014) estimated the price would drop by 25% by 2020 with high production.

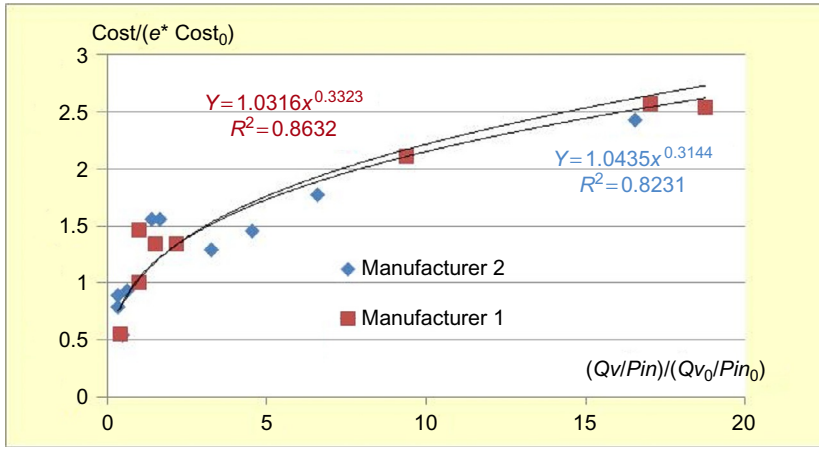

FIG. 6.5 Comparison of the power law for the cost of compressors for two manufacturers, after the trademark effect has been removed.

- On the other hand, when compared with data from Nexant Inc. et al. (2008) (2007), the present correlation gives a higher cost for a 50 kg/h 20–400 MPa 2-stage diaphragm compressor, 308 k$ instead of 170 k$ for the quotation. However, when the flow rate is doubled, the correlation gives the same price as the quotation: 385 k$.

6.3.2 Cost of Pressure Vessels

As for compressor investment cost, some information can be found about high-pressure vessel cost in a number of papers, for example, Parks et al. (2014), Reddi et al. (2014), Nexant Inc. et al. (2008), but no model is available.

- Nexant Inc. et al. (2008) considers large steel vessels of 21 kg H_2 each under 43 MPa for a price of 843 $/kg (2007, uninstalled).
- Reddi et al. (2014) considers 100 MPa steel bottles with a capacity of 12 kg for a rather high cost of 1475 $/kg (2013, +30% for installation).
- Parks et al. (2014) reports previous figures from Nexant Inc. et al. (2008) and adds others, with lower costs and for higher pressure. For 61 kg at 25 MPa, a 5 kg type 4 bottle container is reported at a cost of 450 $/kg (2007) and at 95 MPa, 12 kg type 4 bottles are selected at a cost of 911 $/kg.

It is interesting to note that composite bottles have reached lower cost than steel vessels and will continue to drop in cost with mass production, whereas steel vessels will drop less in cost as the technology is has been mature for a long time.

Three manufacturers of composite type 3 and type 4 pressure bottles were queried in 2015 and 2016. They covered a range of bottles with nominal pressures from 20 to 52.5 MPa and volumes from 75 to 500 L. It was then possible to show that the costs of the composite bottles could fit a correlation based on the nominal pressure and the mass capacity of the bottles of the following form:

$$Cost_{bottle} = c * (p_{nom\ bottle})^{p} * (capa_{bottle})^{m} \tag{6.16}$$

with $p_{nombottle}$ in MPa, $capa_{bottle} = \rho_{H2nombottle} * V_{bottle}$ in kg, $p = 0.27$, $m = 0.875$, and $c = 331€$. When applied to the bottle characteristics of Parks et al. (2014), the correlation gives a price of 635 €/kg = 730 $/kg at 25 MPa and 840 €/kg = 965 $/kg at 95 MPa. Thus, the order of magnitude is correct while the effect of pressure seems to be underestimated.

In fact, in (Parks et al., 2014) at 25 MPa, the bottles were assembled in a container for a larger capacity and the cost should be compared to costs collected by enquiries for containers varying from 160 to 850 kg. The cost of a container made of elementary bottles can be expressed as:

$$Cost_{container} = n^{q} * c' * c * (p_{nom\ bottle})^{p} * (capa_{bottle})^{m} \tag{6.17}$$

where c' is a coefficient relative to the cost of building the frame of the container, the supports of vessels and their connection, with a value of 1.3–1.5 (from quotation analysis, relevant with Nexant Inc. et al., 2008), n is the number of vessels necessary for the container capacity requirement, and the exponent q reveals the number effect, from 0.90 to 0.94 (from quotations analysis from different suppliers). When applied to the 616 kg container of Parks et al. (2014), the correlation gives a cost of 680 €/kg for the assembled container instead of 635 €/kg for a single 5 kg bottle; the number effect has nearly compensated the assembly cost.

These correlations are used in Sections 6.4 and 6.5 without taking into account the cost drop with large quantity production, which will indubitably occur in the coming years.

6.3.3 Preliminary Considerations and Recommendations

At this stage, good practices have already appeared concerning hydrogen compression:

- Use high p_0: as far as possible, produce the hydrogen at the highest pressure, using a high-pressure electrolyzer or a high-pressure reformer and PSA. It is less costly to compress the water feeding the electrolyzer or the biogas at the inlet of the reformer than the hydrogen at the exit. In the VABHYOGAZ project, the reformer operates at $p_0 = 1.5$ MPa.
- Use low T_0: cool the hydrogen before compression, as far as the compressor accepts it. Calculations (see later) show that with a $COP_{cooling}$ of 3, the hydrogen refrigeration will require less electric energy than can be spared when compressing hydrogen at lower temperature.
- Cool the compressor heads effectively so that the compression process is as near as possible to an isothermal process. Consider a multistage compressor with intercooling to lower the compression ratio of each stage and isentropic heating.
- Choose best compression technology: diaphragm compressors are more effective than boosters.
- Prefer large-scale units: it is difficult to reach good compressor efficiency in small production or distribution units.
- Choose an effective cooling system to cool compressor heads and hydrogen.

6.4 CASE OF H_2 DISTRIBUTION ON THE PRODUCTION SITE

When hydrogen production and distribution are located on the same site, there is no transportation to be considered and the energy requirements are mainly from the compression and associated cooling of the hydrogen.

6.4.1 Current Practices for Refueling: Energy Costs for Reference Cases

In the current practice, referring to Fig. 6.2, during the filling of successive vehicle tanks, the buffers numbered 1, 2, and 3 are always connected in the same order to the vehicle and they are then refilled by the compressor in the opposite order, with a priority to the highest-pressure buffer, number 3. Then, when buffer number 3 has recovered its nominal pressure, it is the turn of buffer number 2 to be refilled by the compressor up to its nominal pressure. And finally, it is the turn of buffer number 1 to be refilled. Even though Rothuizen and Rokni (2014) writes that the compressor refills the buffers in the order they are filling the tanks, i.e., number 1 first, this practice seems not to be implemented.

Indeed, refilling the buffer number 3 first is useful for the peak hour performance; this highest-pressure buffer will recover its nominal pressure (45 MPa or 90 MPa) within the shortest time so the probability of the refueling station to have a buffer able to achieve the next tank refueling at the nominal pressure is the highest. Then, a cascade naturally appears in the buffer pressures when cars follow each other at peak hour, but after these peak hours, or during the night, all of the buffers are refilled at the highest pressure.

Using the previous section, and specifically Eqs. (6.8), (6.9), and (6.12), it is now easy to calculate the electric consumption of the compressor and associated cooling of any refueling station. The necessary data are: daily delivering capacity: 80 kg/day, buffers pressure: 45 MPa, production unit working pressure: 1.5 MPa, number of stages of the diaphragm compressor: 2, inlet temperature: 20°C, and finally, cost of electricity: 80 €/MWh. An example of detailed results for this refueling station at nominal load is given in Table 6.1.

TABLE 6.1 Consumption and Cost for Compression and Cooling of 80 kg/Day From a Production Pressure of 1.5 MPa to a Buffer Pressure of 45 MPa

Useful isothermal compression power, real gas (kW)	4.07
Isentropic compression power, real gas (kW)	5.14
Compressor electric consumption ($kW_{élec}$)	8.82
Cooling consumption (kW_{cool})	8.48
Total electric power ($kW_{élec}$)	11.65
Annual electricity consumption (MWh/an)	96
Annual electricity cost (k€/an)	7.69
Specific consumption (kWh/kgH_2)	3.50
Ratio of specific consumption to LHV (% LHV)	10.6
Specific cost ($€/kgH_2$)	0.266

TABLE 6.2 Effect of Capacity and Distribution Pressure of Refueling Station (With OnSite Production) on Electricity Consumption and Cost for Cooled Compression at Nominal Load

Daily Capacity of the Refueling Station (With On-Site Production)	20 kg/Day		80 kg/Day		200 kg/Day	
Distribution pressure (MPa)	35	70	35	70	35	70
Electricity consumption for cooled compression (MWh/an)	28	34.6	96	119	222	275
Specific consumption (% LHV)	12.4	15.2	10.6	13.1	9.8	12.1
Electricity cost (k€/an)	2.24	2.77	7.69	9.53	17.8	22.0

The results show rather high specific energy and specific cost for this reference case, >10% of the LHV. They will be even higher for smaller distribution units, but hopefully lower for larger ones, as given in Table 6.2, which shows also the effect of the delivering pressure: 35 MPa or 70 MPa (with buffers at 45 MPa or 90 MPa).

6.4.2 Minimization of the Compression Energy

6.4.2.1 The Geometric Progression Pressure Cascade

In fact, it is not necessary to use a buffer at the highest pressure during the first moments of the refueling process and it generates a waste of energy; indeed, all the hydrogen has been compressed to the highest pressure, whereas an intermediate pressure would have been sufficient during these first moments.

It has been suggested that the buffer nominal pressures be staged and that the buffers never be refilled at a higher pressure than their respective staged pressures. If vehicles usually have to be refilled when their tank pressure, $p_{0,tank}$, is equal to a fraction, v_{tank}, of their nominal tank pressure, $p_{f,tank}$, with:

$$p_{0,tank} = v_{tank} * p_{f,tank} \tag{6.18}$$

in a refueling station equipped with n buffers, the tank pressure will increase in a ratio $R_p = {}^{1}/_{v_{tank}}$ through n steps, and each step will contribute for a smaller pressure ratio increase r_p :

$$r_p = \left(R_p\right)^{1/n} \tag{6.19}$$

TABLE 6.3 Geometric Progression Staged Buffer Pressures for Different Numbers of Stages for a Refueling at 70 MPa and $v_{tank} = 4\%$

Number of Stages n	Stage Pressure Ratio r_p	Pressure Cascades: Geometric Progression of the Staged Buffer Pressures (MPa)			
$n = 1$	$R_p = {}^1/_v = 25$	90			
$n = 2$	$(25)^{1/2} = 5.0$	18.0	90		
$n = 3$	$(25)^{1/3} = 2.92$	10.53	30.78	90	
$n = 4$	$(25)^{1/4} = 2.236$	8.05	18.0	40.25	90

For a refueling at 35 MPa instead of 70 MPa, just divide the values of pressures by 2.

Then, the buffers form a pressure cascade staged in a geometric progression. For example, for a refueling at 70 MPa, with the highest pressure buffer at 90 MPa and $v_{tank} = 4\%$, the pressure cascades are given in Table 6.3.

It can be noted that for a given mass of perfect gas, n compression steps with the same pressure ratio, r_p, require equal compression energy; according to Eqs. (6.3) and (6.5); the pressure cascade is isoenergy. For a real gas, such as hydrogen, the higher compression steps will require slightly higher compression energy, even with the same r_p.

6.4.2.2 Highlighting of Energy Savings

The effect of a pressure cascade on the energy needs is depicted in Fig. 6.6, which presents the progressive filling of a 70 MPa tank initially empty at $v_{tank} = 4\%$ (corresponding to a residual mass $w_{tank} = 5.8\%$ in the tank):

- With only 1 buffer at 90 MPa, or with all buffers at 90 MPa, according to Eq. (6.8), all hydrogen requires a specific compression energy equal to 3.308 kWh/kg before being transferred to the tank (red curve).
- If 2 staged buffers at 18 and 90 MPa are used, the first 22% of mass transferred to the tank comes from the first buffer at 18 MPa and only requires a specific compression energy equal to 1.525 kWh/kg, while the following 72.2% comes from the second buffer at 90 MPa and requires 3.308 kWh/kg (blue curve).
- If 4 staged buffers are used, at 8, 18, 40.2, and 90 MPa, the first 7% transferred mass comes from the first buffer at 8 MPa and only requires a specific compression energy equal to 0.967 kWh/kg; the following 15% transferred mass comes from the second buffer at 18 MPa and requires an energy equal to 1.525 kWh/kg; the following 28% transferred mass comes from the third buffer at 40.2 MPa and requires an energy equal to 2.236 kWh/kg; while the last 44.2% comes from the fourth buffer at 90 MPa and requires 3.308 kWh/kg (orange curve).

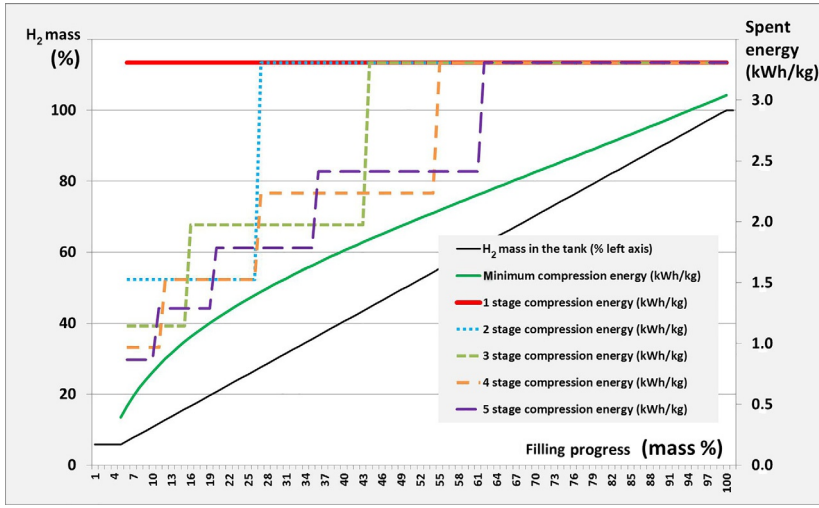

FIG. 6.6 Specific compression energies (kWh/kg) involved in the filling of a 70 MPa hydrogen tank when using buffers arranged in geometric pressure cascades with 2–5 stages, compared to the case of 1 unique very-high-pressure buffer (VHPB) and to the case of an infinite number of staged buffers (minimum energy).

- On this plot, the areas under the stair-shaped lines represent the energies spent for the compression of the hydrogen to be transferred. So, the area between the highest, red, straight line, and the other stair-shaped lines represent the energy saved thanks to the use of pressure cascades with 2, 3, 4, or 5 stages.
- On the opposite side, the green curve shows the minimum compression energy that would be spent with an infinite number of stages and buffers at increasing pressures equal to that of the tank. It is also the energy that would be spent by a compressor connected to the tank and filling it directly. The areas between the stair-shaped lines and that green curve represent the compression energy lost in the process of filling a tank by transfer from higher pressure buffers.

6.4.2.3 Energy Savings as a Function of Number of Stages and Tank Pressure

The areas under the stair-shaped lines have been calculated to obtain the numerical values of the energies shown in Table 6.4 for the filling of a 70 MPa hydrogen tank:

The same calculations have been made for the filling of a 35 MPa hydrogen tank (Table 6.5):

TABLE 6.4 Specific Compression Energies (kWh/kg) Involved for Filling of a 70 MPa Hydrogen Tank, Gains Generated When Using Buffers Arranged in Geometric Pressure Cascades With 2–5 Stages in Comparison With the Case of a Unique Very-High-Pressure Buffer (VHPB) and to the Case of an Infinite Number of Staged Buffers (Minimum Energy)

Number of Stages	1	2	3	4	5	Infinite
Specific compression energy spent (kWh/kg)	3.33	2.94	2.71	2.58	2.51	2.01
Specific compression energy spent/LHV (% LHV)	10.1	8.9	8.2	7.8	7.6	6.1
Losses with respect to minimum energy (%)	66	46	35	29	25	0
Gains with respect to unique pressure buffer (%)	0	11.9	18.8	22.5	24.9	39.8

TABLE 6.5 Same as Table 6.4 but for the Filling of a 35 MPa Hydrogen Tank

Number of Stages	1	2	3	4	5	Infinite
Specific compression energy spent (kWh/kg)	2.65	2.38	2.21	2.12	2.06	1.64
Specific compression energy spent/LHV (% LHV)	8.0	7.2	6.7	6.4	6.2	5.0
Losses with respect to minimum energy (%)	61	45	35	29	25	0.0
Gains with respect to unique pressure buffer (%)	0.0	10.4	16.6	20.2	22.4	38.0

Fig. 6.7 shows the energy saved when using buffers arranged in 2–5 stage geometric pressure cascades in comparison with the current practice in which all buffers are filled at very high pressure.

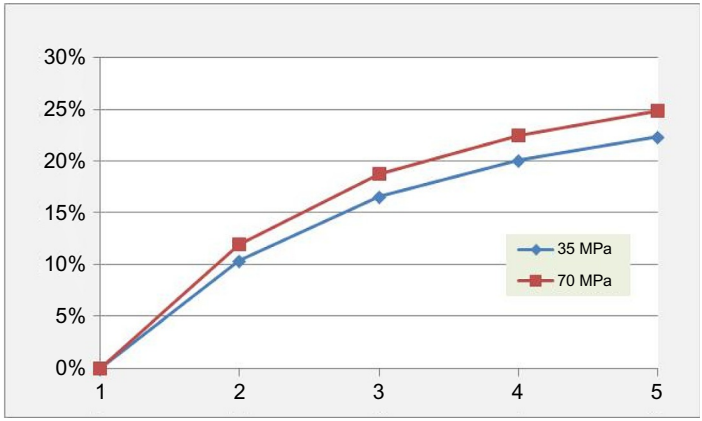

FIG. 6.7 Saved energy when using buffers arranged in geometric pressure cascades with 2–5 stages in comparison with the current practice of all buffers filled at very high pressure (45 or 90 MPa).

6.4.2.4 Effect of the Shape of the Pressure Cascade on the Energy Savings

The previous results have been obtained with pressure cascades organized in geometric progressions. For a perfect gas, these cascades are isoenergy and require isovolume buffers at each cascade stage (see next section). But nothing says that this arrangement will lead to the lowest compression energy.

Thus, the same calculations have been performed for other cascade shapes; arithmetic progressions have been considered, together with combinations of arithmetic and geometric progressions (Table 6.6; Fig. 6.8).

It appears in Fig. 6.8 that an arithmetic progression gives better results than a geometric one and the best results are obtained with a linear combination of 0.3

TABLE 6.6 Arithmetic Progression Staged Buffer Pressures as Function of Number of Stages for a Refueling at 70 MPa

Number of Stages *n*	Pressure Increase (MPa)	Pressure Cascade: Arithmetic Progression of the Staged Buffer Pressures (MPa)			
$n=1$	90	90			
$n=2$	90/2 = 45	45	90		
$n=3$	90/3 = 30	30	60	90	
$n=4$	90/4 = 22.5	22.5	45	67.5	90

For a refueling at 35 MPa instead of 70 MPa, just divide the values of pressures by 2.

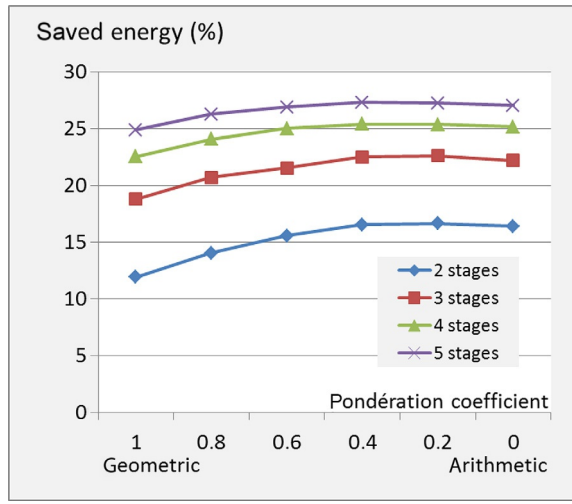

FIG. 6.8 Influence of the shape of the pressure cascade, from a geometric progression to an arithmetic progression, with 2–5 stages, on the saved energy for a 70 MPa distribution.

geometric +0.7 arithmetic progression, but the variations are rather flat, leaving a large possibility for energy savings higher than 25% in comparison with the current practice where all buffers are filled at the highest pressure (90 MPa).

An additional point of interest of lower pressure buffers for the early stages of refueling is to minimize the pressure ratio of the Joule-Thomson expansion occurring in the control valve of the refueling line and to minimize the temperature rise. With 10 MPa in place of 90 MPa, the Joule-Thomson temperature rise is 40 K lower, thus reducing the cooling need!

At this stage, a comparison with similar previous approaches is interesting. Rothuizen and Rokni (2014) is dedicated to the optimization of the energy consumption in cascade refueling. Its detailed modeling reports an energy consumption (compression + cooling) of 5.97 kWh for refueling 5 kg in a 70 MPa tank (3.6% of LVH_{H2}) with 1 stage and a decrease to 5 kWh with 2 stages (−16.2%) and to 4 kWh with 5 stages (−33%). Similar to the present study, the largest saving comes from the lower output pressure for the compressor; similar to Fig. 6.7, the shape of the curves shows that the first stages bring most of the savings while the 5th and higher stages bring smaller and smaller contributions. But it is difficult to go further in the comparison because Rothuizen and Rokni (2014) considers a refueling station supplied from a bulk storage at a higher pressure than the present 1.5 MPa (more comparable with cases treated in Section 6.5.3) and this explains the low energy demand, 3.6% of LHV_{H2}, not including the compression on the production site. Then, our saving, 24.9% of 12.1% of LHV_{H2} (Tables 6.2 and 6.4), is 3% of LHV_{H2} and is much more than the saving of 33% of 3.6% of LHV_{H2} (=1.2% of LHV_{H2}) calculated in Rothuizen and Rokni (2014).

6.4.3 Effect of Precooling on the Compression Energy

Considering Eqs. (6.3) or (6.4), another possibility to decrease the compression work is to decrease T_0 by cooling the hydrogen before compression. Calculations show that both the compression work and the compression cooling energy decrease, respectively, by −11 Wh/kg°C and −7 Wh/kg°C. Indeed, it is necessary to take into account also the initial precooling (+7.4 Wh/kg/°C), which cancels the gain of the final cooling. But globally, with a COP of 3, an overall saving of 10.6 Wh/kg/°C can be reached; thus, 0.22 kWh/kg can be saved for a cooling of 20°C at the entrance of the compressor, and this is an extra 5% energy savings, as shown in Table 6.7.

Thus, it is recommended to run the compressors with precooled hydrogen, at the lowest temperature possible, according to the compressor requirements.

6.4.4 Necessary Volume of the Buffers

The delivery capacity of a refueling station at the peak hour mainly relies on the mass of hydrogen stored in the HP buffers. Now, if the buffers are not all at the highest pressure, but are organized in a pressure cascade, their volume has to

TABLE 6.7 Effect of Hydrogen Precooling on Consumption for Compression and Cooling of 80 kg/Day from a Production Pressure of 1.5 MPa to a Buffer Pressure of 90 MPa

Compressor Inlet Temperature (°C)	20	0	−20	Variation
Compressor electric consumption ($kW_{élec}$)	11.03	10.30	9.57	
Specific variation (Wh/kg°C)				−11
Inter and final cooling needs (kW_{cool})	10.16	9.69	9.22	
Specific variation (Wh/kg°C)				−7.0
Initial cooling needs (kW_{cool})	0	0.53	1.06	
Specific variation (Wh/kg°C)				+7.4
Total electric power ($kW_{élec}$)	14.42	13.71	12.99	
Specific variation (Wh/kg°C)				10,6
Specific energy (kWh/kgH_2)	4.33	4.11	3.90	
Specific energy to LHV ratio (% PCI)	13.1	12.5	11.8	
Energy saved (%)	0	5	10	

be increased or else the peak hour performance will be reduced. Then, the investment cost of the staged buffers could be higher than that of smaller HP buffers. This section calculates the volume of the necessary buffers and estimates their investment cost in order to compare overinvestment and energy savings and to quantify the return on investment (ROI). But first the peak demand is defined.

6.4.4.1 Peak Hour Demand and Buffer Capacity

The demand at a refueling station is not constant. It varies with the day and with the week. The result of a statistical treatment of 385 US refueling stations is presented in Nexant Inc. et al. (2008), from which the data of Fig. 6.9A and B are extracted and analyzed here:

- Friday is the busiest day of the week, with a demand 7.5% above the average, while Monday is the quietest day.
- 3 p.m. is the busiest hour in the day with, on Friday, 7.8% of the total of the day, or 1.87 times the average of the day.
- 7 a.m. and 7 p.m. are on the Friday daily average, while the 12 h period in between is above the average; thus, it appears there is no peak hour but a large peak period.
- The area above the average line represents 27.5% of the total area (Fig. 6.9).

The minimum capacity for the HRS compressor would correspond to the average flowrate, with a 24 h/day operation. Then it will be necessary for the buffer to contain an extra mass of hydrogen, deliverable at the desired pressure, equal to 27.5% of the daily dispensed hydrogen. During the period 7 a.m. to 7 p.m., destocking hydrogen will occur from the buffer and its pressure will decrease down to the minimum acceptable pressure. After 7 pm, the hydrogen dispensed to the vehicle tanks is less than the average and the compressor delivers more than what is dispensed to the vehicles, thus stocking in the buffer will occur and its pressure will increase. The compressor will refill the buffer at its nominal pressure until 7 a.m., with an extra mass equal to 27.5% of the daily hydrogen dispensed.

In fact, it is recommended to oversize the compressor to be able to cope with some extra affluence, invisible in the average statistics. With a higher capacity compressor, the buffer will recover its nominal pressure sooner and then the compressor will stop, so that it will operate <24 h/day.

Also, when dealing with small capacity HRSs, dedicated to small captive fleets, the refueling behavior may be different and the delivery profile of the station has to be defined carefully in order to adjust the peak hour performance.

The following calculations consider a *compressor oversized by a factor of 2* and a mass of hydrogen that can be dispensed at the nominal delivery pressure during the peak hour or period, m_{peak}, *equal to 25% of its daily capacity* (i.e., $m_{peak} = 20$ kg for an 80 kg/day HRS). Thus, the compressor only runs 12 h/day

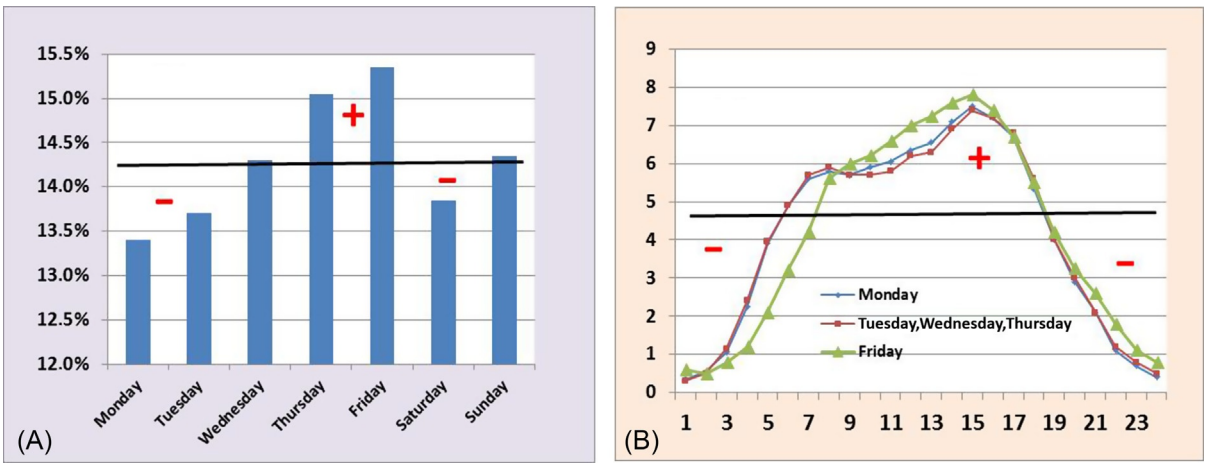

FIG. 6.9 Average hourly (A) and daily (B) gasoline distribution profile. *((Data from Nexant Inc., Air Liquide, Argonne National Laboratory, Chevron Technology Venture, Gas Technology Institute, National Renewable Energy Laboratory, Pacific Northwest National Laboratory, TIAX LLC, May 2008. H2A: Hydrogen delivery infrastructure analysis models and conventional pathway options analysis results. Report DE-FG36-05GO15032, DOE. www1.eere.energy.gov/hydrogenandfuelcells/pdfs/nexant_h2a.pdf.))*

on average and with such a value of m_{peak}, it is possible to face 3 h of peak demand at 8% of the daily average without the help of the compressor. With the help of the compressor, capable of delivering 8.33% of the daily capacity per hour, the buffer will have recovered its nominal pressure at the end of the most demanding hour. In fact, the *maximum capacity of the refueling station is twice its nominal capacity* and the vehicle fleet can increase by a factor of 2 before the station is overwhelmed.

6.4.4.2 Analytical Formulation of Buffer Volumes

The mass of hydrogen, m_{peak}, that can be delivered at the nominal pressure (35 or 70 MPa) is now defined and this mass corresponds to a volume $V_{peak:}$

$$V_{peak} = {}^{m_{peak}}/_{\rho_{H2,tank}} \tag{6.20}$$

Tanks of volume V_{peak} have to be refilled from $p_{tank,0}$ to $p_{tank,f}$ with m_{peak} while the buffer pressure decreases from $p_{buff,0}$ to $p_{tank,f}$. Besides R_p, the tank filling pressure ratio, a new pressure ratio is introduced, S_p, the overpressure of the initial full buffer with respect to the objective full tank pressure:

$$R_p = {}^{p_{tank,f}}/_{p_{tank,0}} = {}^{1}/_{v_{tank}} \tag{6.21}$$

$$S_p = {}^{p_{buff,0}}/_{p_{tank,f}} \tag{6.22}$$

Considering the mass conservation during the balancing of pressures between buffer and tanks and a perfect gas, the volume of the buffer, V_{buff}, necessary to fill the tank volume, V_{peak}, in a pressure ratio, R_p, with a buffer overpressure, S_p, can be calculated as:

$${}^{V_{buff}}/_{V_{peak}} = {}^{(R_p-1)}/_{[R_p*(S_p-1)]} \tag{6.23}$$

It should be noted when writing Eq. (6.17), that the balancing of pressure is supposed to be isothermal, whereas compression occurs in the tank and heats hydrogen and expansion occurs in the buffer. Thus Eq. (6.17) is only valid after tank and buffer have recovered their initial temperature.

Now the flow of hydrogen is not conducted until the exact isothermal balancing of pressure, because it would be long. In fact, taking into account the temperature rise in the tank during the refueling, it is necessary to fill the tank with an overpressure so that, after the tank has cooled down to ambient temperature, the pressure has decreased to the desired $p_{tank,f}$.

So, it is considered that the tanks must be refilled while the buffer pressure decreases to $p_{buff,f,min}$, keeping a minimum overpressure $s_{p,min}$:

$${}^{p_{buff,f,\min}}/_{p_{tank,f}} = s_{p,\min} \tag{6.24}$$

Then, the volume of the necessary buffer is calculated as:

$$V_{buff}/V_{peak} = (R_p - 1) \Big/ \left[R_p * \left(S_p - s_{p,\min}\right)\right] \tag{6.25}$$

Moreover, hydrogen is not a perfect gas and a correction has to be introduced as a ratio of compressibility factors:

$$V_{buff}/V_{peak} = \left[Z_{p_{buff},0}/Z_{p_{tank,f}}\right] * (R_p - 1) \Big/ \left[R_p * \left(S_p - s_{p,\min}\right)\right] \tag{6.26}$$

Finally, Eq. (6.26) allows the volume of the necessary buffer for the peak hour demand to be estimated easily, without detailed modeling of the unsteady filling of the tank, including hydrogen heating and heat transfer to the tank walls, as done in Rothuizen and Rokni (2014) and Reddi et al. (2014). In fact, all the thermal behavior of hydrogen and tank is represented by the factor $s_{p,min}$. According to the SAE-J2601 standard (SAE International, 2014), to compensate the heating of the hydrogen and tank, it is possible to overfill the tank (over its nominal pressure), so that after the natural cooling, its pressure decreases to its nominal pressure. Target pressures with a 1.10 overpressure factor are current when fueling at high ambient temperature (e.g., a target of 77.9 MPa for the refueling end for a nominal 70 MPa after natural cooling). Thus, using a $s_{p,min} = 1.1$ in Eq. (6.26) assumes that the pressure can increase by a factor 1.1 in the tank due to the hydrogen temperature increase in the same ratio, an increase from 290 to 320 K, which is rather low, and would mean that hydrogen has been cooled before entering the tank. Without precooling, the hydrogen temperature would be higher (but under 85°C), and either $s_{p,min}$ should be chosen higher than 1.10 to keep good peak hour performance, or the flow rate should be decreased in order to decrease the hydrogen temperature.

Thus, as long as $s_{p,min}$ is correctly estimated, there is no necessity of detailed thermal modeling, nor to consider filling rate, tank filling duration, or time between two successive vehicles…

Now, to estimate correctly $s_{p,min}$, information can be gained from detailed transient heat transfer modeling inside the tank and Bourgeois et al. (2015, 2017), Lei et al. (2010), Woodfield et al. (2007), Monde et al. (2007), and Lee et al. (2009) will be useful, especially Bourgeois et al. (2017) for the model description, and Lei et al. (2010) for results concerning the temperature rise as a function of filling rate, initial tank pressure, and ambient temperature.

6.4.4.3 Buffer Volume With Only 1 Very-High-Pressure Buffer (VHPB) at the Highest Pressure 45 MPa or 90 MPa (Reference Case)

For an 80 kg/day refueling station, $m_{peak} = 20$ kg; with $\rho_{H2,tank} = 24$ kg/m^3 at 35 MPa or 40.24 kg/m^3 at 70 MPa, V_{peak} is obtained: $V_{peak,\ 35MPa} = 0.833$m^3 and $V_{peak,70MPa} = 0.497$m^3. $R_p = 25$ for $v = 4\%$ and $S_p = 1{,}285$ for $p_{buff,0} = 90$ MPa and $p_{tank,f} = 70$ MPa or for $p_{buff,\ 0} = 45$ MPa and $p_{tank,f} = 35$ MPa, thus, following Eq. (6.26): $V_{buff}/V_{peak} = 5.48$ and finally: $V_{buff,45MPa} = 4.56\ m^3$, $V_{buff,90MPa} = 2.72\ m^3$.

TABLE 6.8 Volume of Necessary Buffers in Case of Geometric Progression Staged Buffer Pressures

Number of Stages n	Stage Pressure Ratio r_p	V_{buff}/V_{peak} for Each Stage
$n=1$	$r_p=R_p=25$	5.48
$n=2$	$r_p=(25)^{1/2}=5.0$	4.57
$n=3$	$r_p=(25)^{1/3}=2.92$	3.76
$n=4$	$r_p=(25)^{1/4}=2.236$	3.16
$n=5$	$r_p=(25)^{1/5}=1.903$	2.71

6.4.4.4 *Buffer Volumes With Staged Pressure*

In the case of staged pressure buffers, the approach is formally the same and the only difference in the formulas is the substitution of the overall large pressure ratio, R_p, by the smaller pressure ratio, r_p, of each stage.

If the buffer pressures are staged in a geometric progression, all r_p are equal and then the buffer volumes are equal at each stage; the volumes are given in Table 6.8. It is clear that each stage requires a smaller volume of buffer, but globally, the total volume of buffers is larger.

6.4.5 Cost of the Storage Buffers

If all buffers are designed for the highest pressure, as in Rothuizen and Rokni (2014) or Reddi et al. (2014), the investment cost of the buffers will be higher. But as the lower pressure buffers will never experience the highest pressure, they can be designed for lower pressure; the overinvestment could be small.

Yet, composite bottles are only available for a few capacities and a few nominal pressures. The commercially available nominal pressures do not respect a geometrical progression (but they could lead to better energy savings as shown in Fig. 6.6). Adequate staged volumes have to be calculated as a function of each pressure ratio according to Eq. (6.20); they do not have equal values and furthermore will not correspond to the commercially available volumes. Thus, some buffers will have to be oversized, inducing additional cost.

It is considered here that bottles are available only with a unit volume of 300 L and for nominal pressures of 10, 20, 30, 52.5, and 90 MPa. The number of necessary 300 L bottles is calculated in Table 6.9 for each stage of the storage of an 80 kg/day 70 MPa refueling station. The cost of the storage is then obtained, using Eq. (6.10). The saving percentage is obtained from Fig. 6.8.

It can be seen that:

- In the reference case of current practice, with one only very-high-pressure stage (90 MPa), 6 bottles of 300 L would be needed (exact theoretical total

TABLE 6.9 Effect of Number of Stages on Number of Bottles of 300 L Needed at Each Stage, Cost of Storage, Energy Savings and Return on Investment for an 80 kg/Day 70 MPa HRS

Number of Stages	1	2	3	4	5
10 MPa buffer number					3
20 MPa buffer number				4	3
30 MPa buffer number		6	5	3	3
52.5 MPa buffer number			3	3	3
90 MPa buffer number	6	4	3	3	3
Storage cost (k€)	63.0	66.1	72.6	75.5	76.8
Annual energy savings (%)	Reference	16.0	22.4	25.2	26.3
Annual energy savings (k€)	Reference	1.52	2.13	2.40	2.51
Return on investment (years)	Reference	2.0	4.5	5.2	5.5

volume needed is 1816 L) for a total cost of 63 k€; the annual operation reference cost of energy is 9.53 k€/year, according to Table 6.2.

- With 2 stages, when introducing an intermediate 30 MPa stage, 4,300 L 90 MPa bottles would be enough (theoretical volume needed is 1263 L) together with 6,300 L 30 MPa bottles (theoretical volume needed 1663 L); the total cost is 66.1 k€ and the energy saving is 16% with respect to the reference case; thus, the return on investment is only 2 years.
- With 4 stages, introducing intermediate stages at 14.5 MPa, 30 MPa, and 52.5 MPa, 3,300 L 90 MPa bottles would be used, (even if too large, the theoretical volume needed is 793 L) together with 3,300 L 52.5 MPa bottles (theoretical volume 809 L), 3,300 L 30 MPa bottles (theoretical volume 979 L) and 4,300 L 20 MPa bottles (theoretical volume 1479 L); the total cost is 75.5 k€ and the energy saving is 25.2%, thus the return on investment is 5.2 years.
- The use of staged pressure buffers increases the total storage volume and the investment cost. The overinvestment payback time increases with the number of stages but remains acceptable.

6.4.6 Conclusion for Hydrogen Distribution on the Production Site

Compressing hydrogen is inevitable when fuel cell cars have to be refueled at high pressure. The energy cost of compressing and cooling hydrogen is high. In the case of hydrogen dispensed on the production site, it can reach *3.50 or 4.4 kWh per kg* of hydrogen transferred to the car tank at *35 or 70 MPa*, in a

reference case corresponding to best current practice. Recommendations have been made in order to avoid spending even more energy, which is current in small refueling stations.

The study shows that this energy need can be reduced by *22%*, *25%*, or even *27%* when judiciously using *3*, *4*, or *5* stages of buffers organized in a pressure cascade for the filling of the tank. Whereas the total volume of the staged pressure buffers is higher than the volume of a unique very-high-pressure buffer, the extra cost is acceptable and the energy saving results in an acceptable payback time for the overinvestment of *4.5 to 5.5 years*.

Precooling the hydrogen before the compression would also lead to energy savings; an extra *5% to 10%* can be gained, and compressor technology could be improved to admit cooled hydrogen.

6.5 CASE OF A PRODUCTION UNIT SUPPLYING SEVERAL DISTANT REFUELING STATIONS

Currently, most of the hydrogen dispensed is supplied from large and distant production units: only a few HRSs have onsite production.

Hydrogen is usually supplied in steel bottle bundles or trailer tubes, which are trucked to the station. These steel containers have a low specific content with a bundle of 12 steel 50 L 20 MPa bottles weighing 1010 kg for a content of 9 kg H_2 only, or a payload of only 0.9%! A trailer with 14 steel 1535 L 20 MPa tubes weighs 31 t for a content of 320 kg H_2, a 1.04% payload!

Transportation energy costs are high as distances between production units and refueling stations can be long and the tractor and its trailer are heavy and greedy. A 38 t hauler can need 35 L of diesel fuel per 100 km. Then, for 320 kg_{H2} of a tube trailer, with 9.85 kWh/L_{Diesel}, and 0.270 kg_{CO2}/kWh_{Diesel}, it is 2.15 kWh/kg_{H2}, 6.5% of LHV_{H2}, and 0.6 t_{CO2}/t_{H2} for each 100 km of distance between production and distribution! And even much more for bottle bundles!

6.5.1 Potential for Reducing Energy Demand

When the production unit supplies hydrogen to several distant refueling stations, energy for transportation by truck and for recompression on the distribution site must be considered, but the distribution unit works in the same way as when on the production site (Fig. 6.2). Potentials explored in this paper to lower the energy spending *of actual or near-future small refueling stations* are:

- reduce the distances between production units and distribution sites to a 50 km average.
- use small transportable containers of high-pressure light composite bottles at 30, 50 MPa or even more, when available.
- use these transportable containers in place of intermediate pressure buffers on the distribution site (Fig. 6.10).

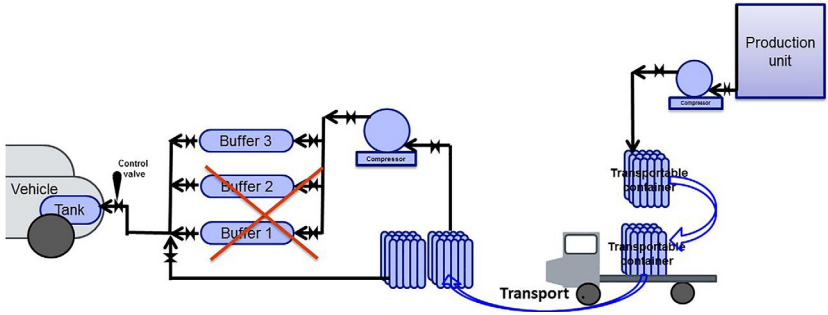

FIG. 6.10 Schematic view of the equipment for filling the HP tank of a hydrogen vehicle in a refueling station supplied by truck from a distant hydrogen production unit.

6.5.1.1 *Distributed Hydrogen Production to Reduce Transportation Distance*

Reducing the hydrogen transportation distance to about 50 km (always <100 km) is a specific possible advantage of distributed hydrogen production, promoted by the VABHYOGAZ3 project, which considers hydrogen production from biogas. As biogas can be produced from many kinds of waste and in lots of places, hydrogen refueling stations will never be far from a hydrogen source. This is also the case for hydrogen production from an electrolyzer. To the contrary, it is not the case in the current practice as hydrogen is now mainly produced by steam reforming in large units located, for example, on refinery sites, and hydrogen transportation distances can then be very long, sometimes >500 km, with 10 times more energy spent and CO_2 emissions for transportation!

6.5.1.2 *Small High-Pressure Light Composite Bottle Transportable Containers*

The use of high-pressure composite bottle containers for hydrogen transportation, in order to reduce transportation cost and energy, has been suggested for a long time. Nexant Inc. et al. (2008) considers 7000 psi (48 MPa) trailers with a capacity of 1000 kg H_2, as does the NREL report (Wipke et al., 2012) which considers a tube trailer at 35 MPa with a capacity of about 800 kg. Commercial offers can be obtained for containers at 25 or 30 MPa (as reported in Section 6.3.2), but these containers are currently only used for natural gas transportation. European Commission programs have promoted developments in this field, but only a few prototypes have been realized, and the current practice still involves 20 MPa steel tube trailers with a capacity around 300 kg, or bundles of steel bottles for smaller quantities. This paper, in the frame of the VABHYOGAZ3 project, *considers the near future (as soon as 2018)*, with smaller production units and smaller refueling stations, and so it considers also

smaller containers from 20 to 200 kg H_2 made of composite bottles with a working pressure of 30 or 52.5 MPa, which can be made available in the near future. The objective is to multiply by >3 the payload in transportation.

6.5.1.3 Optimized Use of the Transportable Containers to Fill Vehicle Tanks

The use of a trailer as the first stage of the pressure cascade for vehicle tank filling (by bypassing the compressor) has already been considered. Reddi et al. (2014) simulates the tube trailers as the first stage of refueling as long as the pressure is over 5 MPa and shows a decrease in the compressor flow rate and storage cost for large stations (250 kg/day). But this does not seem to be the current approach. And if the NREL report (Wipke et al., 2012) finally recommends the use of "low-pressure" bulk storage as a first stage in the cascade filling, this concerns in fact a fixed storage for a production site distribution or for a pipeline supplied distribution.

This paper differs from Reddi et al. (2014) as it considers smaller stations (20–200 kg/day) and the use of small transportable containers for several stages of the pressure cascade, so that just a small very-high-pressure buffer (VHPB) is to be kept and only a small part of the hydrogen is to be compressed to this VHPB.

The question is the level of investment in composite transportable bottles and the resulting overall cost for compression, storage, and transportation of the delivered hydrogen. This section estimates that overall cost, together with the overall energy expenditure, the energy savings and the green gas emissions, and makes comparisons to current practices.

6.5.2 Compression on the Production Site

On the production site where the transportable storage containers are filled, the nominal power for compression and associated cooling can be calculated using Eqs. (6.4), (6.7), (6.8), and (6.13), as in Tables 6.1 and 6.2, taking into account the hydrogen production pressure $p_{prod} = 1.5$ MPa and the storage pressure $p_{sto,0} = 20$, 30, or 52.5 MPa. The production unit is assumed to be running at nominal charge for 8120 h/year, and the compressor does also. But it does not always work at its nominal power. Beginning with empty storage containers at a return pressure $p_{sto,f} = 2$ MPa, the lower pressure ratios induce energy savings, as already noticed in Rothuizen and Rokni (2014). These energy savings are estimated according to Appendix 1 and a reduction coefficient is introduced in Table 6.10. The investment cost of the compressor is estimated according to Eq. (6.15) and a global cost for compression can be calculated assuming a lifetime for the compressor of 8 years, together with an annual maintenance cost equal to 8% of the investment cost.

TABLE 6.10 Energy Spent and Compression Cost for Cooled Compression on Production Site, as Function of the Production Unit Capacity and of the Transportable Storage Pressure (Hydrogen Production Pressure 1.5 MPa, Initial Storage Pressure 2 MPa)

Production Unit Capacity (kg/Day)	100			200			400		
Storage pressure (MPa)	20	30	52.5	20	30	52.5	20	30	52.5
Compressor nominal electric power ($kW_{él}$)	9.1	10.8	13.5	16.9	20.2	25.2	31.6	37.7	47.0
Cooling nominal power (kW_{cool})	8.9	10.6	13.0	16.6	19.7	24.1	31.0	36.6	44.9
Reduction factor for progressive filling	0.71	0.73	0.75	0.71	0.73	0.75	0.71	0.73	0.75
Electricity consumption for cooled compression (MWh/an)	70	85	145	130	159	204	243	296	380
Electricity cost (k€/an)	5.6	6.8	8.7	10.4	12.7	16.3	19.4	23.7	30.4
Specific consumption for cooled compression (kWh/kg_{H2})	1.91	2.33	2.99	1.78	2.18	2.79	1.66	2.03	2.60
Specific consumption for cooled compression (% PCI)	5.7	7.0	9.0	5.3	6.5	8.4	5.0	6.1	7.8
Compressor investment cost (k€)	140	146	155	173	180	190	213	222	235
Global cost for compression and cooling (€/kg H_2)	0.90	0.96	1.05	0.59	0.64	0.70	0.40	0.43	0.49

Compression on the production site benefits from the scale effect; the higher the flow rate, the better the efficiency of the compressor and the lower the specific investment cost of it. Thus, the compression specific cost for hydrogen decreases significantly when increasing the production unit size, −55% for 400 kg/day with respect to 100 kg/day.

6.5.3 Compression on the Distribution Site

On the distribution site, the compressor power can be calculated if all the daily distributed hydrogen is assumed to be recompressed from the transportable storage pressure $p_{sto,0} = 20$, 30, or 52.5 MPa, to the high-pressure buffers at $p_{buff} = 45$ or 90 MPa, as it is usual in the current practice (Reddi et al. 2014).

Again, the compressor will start at lower pressure ratios, which induces energy savings estimated according to Appendix 2, and a reduction coefficient is applied to the electric energy demand.

Moreover, the use of the transportable containers as first stages for direct filling of the vehicle tank reduces the quantity of hydrogen to be compressed to the higher buffer pressure. Thus, the nominal flow rate of the compressor is reduced by a "bypass coefficient" (with respect to the daily distribution capacity) to be estimated as a function of the utilization strategy of the transportable containers, detailed in the following sections.

Table 6.11 gives the reference values of the current practices, namely, storage pressure of 20 MPa, with the first reduction factor, but without the second, as no bypass of the compressor is considered yet.

It can be seen that for small HRSs, with the current practice, the cost of compression can be very high, higher that the cost of compression in the production unit, even if the compressor power is lower.

The next sections discuss how improved container utilization scenarios can lower compressor investment cost and energy demand when using 30 MPa and 52.5 MPa storage containers.

6.5.4 Scenarios for Transportable Container Utilization

The idea is to place several transportable containers on the distribution site and to use them, much as they are, as first stages for filling vehicle tanks, while the compressor takes hydrogen in the lowest-pressure container, compresses it, and fills a higher-pressure buffer. This unique buffer allows the vehicle tank filling to be completed to its nominal pressure.

In the case in which the transportable containers have a nominal pressure higher than the vehicle tank nominal pressure (i.e., $p_{sto} = 52.5$ MPa for $p_{tank} = 35$ MPa), the compressor in no longer necessary, nor is the highest-pressure buffer. This case results in a drastic simplification of the refueling station with a considerably reduced investment and an energy consumption that is also drastically reduced. This case is considered first.

TABLE 6.11 Reference Values for Current Practices: Energy Spent for Cooled Compression on the Distribution Site, for Initial Storage Pressure of 20 MPa, Final Storage Pressure 2 MPa, and Compression of all the Hydrogen to the Buffer Pressure

Refueling Station Capacity (kg/Day)	20		80		200	
Buffer pressure (MPa)	45	90	45	90	45	90
Compressor nominal electric power (kW_{el})	4.75	6.25	16.5	21.8	37.7	49.6
Cooling nominal power (kW_{cool})	4.58	5.85	15.9	20.2	36.1	45.6
Reduction factor for progressive emptying	0.50	0.59	0.50	0.59	0.50	0.59
Electric consumption for cooled compression (MWh/an)	13.7	21.2	48	74	109	168
Electricity cost (k€/an)	1.1	1.7	3.8	5.9	8.7	13.4
Specific consumption for cooled compression (kWh/kg_{H2})	1.88	2.9	1.63	2.52	1.49	2.30
Specific consumption for cooled compression (% LHV)	5.6	8.7	4.9	7.5	4.45	6.87
Compressor investment cost (k€)	104	111	157	168	207	222
Global cost for compression and cooling (€/kg H_2)	3.07	3.36	1.24	1.39	0.70	0.81

6.5.4.1 Refueling at $p_{tank} = 35$ MPa With Storage Containers at $p_{sto} = 52.5$ MPa

With storage at a higher pressure than the tank to fill, the compressor is of no use, but it is necessary to dispose of several storage containers on the distribution site, and these containers will have to be returned to the production unit with a nonnegligible residual hydrogen pressure.

An analytical formulation has been developed to calculate this residual pressure and it is presented in Appendix 3. The result depends on the number of

storage containers present on the distribution site. It is easy to understand that with only one available storage container, this one will not be able to ensure a complete 35 MPa tank filling as soon as its pressure is lower than 35 MPa, or even lower than 38.5 MPa to take into account the heating of hydrogen during filling ($s_{p,min} = 1.10$). So, it should be substituted by another one and returned to the production unit with a residual pressure of $p_{sto,f,1} = 38.5$ MPa, i.e., $v_{sto,1} = 73.3\%$. With a second storage container available, this first one can be further used as a first stage for tank filling and its residual hydrogen pressure will then depend on the filling state of the vehicle tank v_{tank}.

The results are given in Table 6.12 as a function of the number of containers on the distribution site, which is the number of stages in the refueling, for $v_{tank} = 5\%$ ($p_{tank,0} = 1.75$ MPa). Table 6.12 also gives the contribution of each stage to refueling (percentage of tank filling). In the case in which the average v_{tank} is higher, the values of $v_{sto,n}$ would be higher.

Even with 4 stages, the residue returned to the production unit is high, $v_{sto,4} = 16.7\%$, but the advantages are that 100% of the energy mentioned in Table 6.11 is saved and the compressor and buffer investment costs are also saved.

6.5.4.2 *Refueling at* p_{tank} *=35 MPa With Storage Containers at* p_{sto} *=30 MPa*

With storage containers at $p_{sto} = 30$ MPa, it is necessary to use a compressor, which will increase the pressure of a fraction of the hydrogen to fill a buffer at $p_{buff} = 45$ MPa. The analytical equations to calculate this fraction, together with the energy saving, have been formulated and are presented in Appendix 4. The results depend again on the filling state of the vehicle tanks, $v_{tank} = 5\%$, but the residual hydrogen pressure with which the containers are returned to the production unit can now be chosen and are here $v_{sto,f,n} = 6.67\%$, or $p_{sto,f,n} = 2$ MPa.

In Table 6.13 column 2, the fraction of hydrogen to be compressed is shown (on a total of $(1 - v_{tank}) = 95\%$) and this number allows sizing a smaller compressor for the distribution unit; its capacity can be reduced by a factor of 2.5–3 with 3 or 4 stages. The columns 3, 4, and 5 give the contributions of the previous stages to the refueling and the pressure at which the storage is shifted to the lower stage. The last column gives the reduction factor in the energy demand with respect to the reference case in which 20 MPa storage containers would be completely transferred to the high-pressure buffer. It can be noticed that even with 1 available storage container only, it is possible to organize a direct connection for a prefilling of the tank before completing the refueling from the buffer.

Other calculations have been made for $p_{tank} = 70$ MPa and $p_{sto} = 52.5$ and 30 MPa. Because of the greater difference between tank and storage pressures, the contribution of the compressor is higher and the energy saving lower. But the compressor capacity can still be reduced, by a factor of 1.5–2.5.

TABLE 6.12 Effect of the Number of Available 52.5 MPa Storage Containers: Contribution of Each Stage to the Refueling at $p_{tank} = 35$ MPa, Starting With $v_{tank} = 5\%$; Residual Pressure for Each Stage and Residual Fraction Returned to the Production Unit

Number of Storages n	Stage n $p_{sto,f,1}$ $\Delta v_{tank,1}$	Stage $n-1$ $p_{sto,f,2}$ $\Delta v_{tank,2}$	Stage $n-2$ $p_{sto,f,3}$ $\Delta v_{tank,31}$	Stage $n-3$ $p_{sto,f,4}$ $\Delta v_{tank,4}$	Residual Fraction Returned to Production $v_{sto,n}$ (%)
1	38.5 MPa 95%				73.3
2	38.5 MPa 43.3%	21.8 MPa 51.7%			41.5
3	38.5 MPa 33.9%	25.4 MPa 31.6%	13.3 MPa 29.5%		25.3
4	38,5 MPa 30.4%	26.7 MPa 25.5%	17.0 MPa 21.3%	8.8 MPa 17.8%	16.7

6.5.5 Detailed Characteristics and Costs for 20 kg/Day Distribution Units

A detailed example is given; named p_100_d_20, it considers five small distribution units of 20 kg/day within a distance of 50 km of their supplying production unit. The technical details and costs are analyzed and compared in three cases in Table 6.14:

(a) steel 20 MPa storage, 1 stage, no compressor bypass (reference case);
(b) 4 stages 30 MPa composite storage;
(c) 4 stages 52.5 MPa composite storage.

6.5.5.1 Cooled Compression

It appears that for a distribution at 35 MPa, the global cost for cooled compression is reduced by 28% and spent energy and CO_2 emissions are reduced by 55% in case b (30 MPa storage containers) compared to case a (20 MPa reference). They are reduced to 0 in case c (52.5 MPa storage containers). In case b, the nominal power of the compressor is much lower as a large fraction of hydrogen can bypass it, and so are the consumption and CO_2 emissions (green-house gas emissive power of French electricity is taken at 60 g_{CO2}/kWh_{el}).

TABLE 6.13 Effect of the Number of Available 30 MPa Storage Containers; Stage n is connected to the compressor; $p_{sto,f,n} = 2$ MPa; contribution of each stage to the refueling at $p_{tank} = 35$ MPa, starting with $v_{tank} = 5\%$; residual pressure for each stage and reduction factor for the compressor energy demand

Number of Storages n	Stage n (Compressor) $p_{sto,f,1}$ $\Delta v_{tank,1}$	Stage $n-1$ $p_{sto,f,2}$ $\Delta v_{tank,2}$	Stage $n-2$ $p_{sto,f,3}$ $\Delta v_{tank,31}$	Stage $n-3$ $p_{sto,f,4}$ $\Delta v_{tank,4}$	Energy Demand Reduction With Respect to Reference Case
1	2 MPa 75%	2 MPa 20%			0.75
2	2 MPa 53,7%	17.8 MPa 41.3%			0.591
3	2 MPa 40,3%	23.3 MPa 23.7%	13.9 MPa 31.0%		0.480
4	2 MPa 34%	25.4 MPa 15.6%	19.4 MPa 20.4%	11.5 MPa 24.9%	0.359

Nevertheless, for such small distribution units, the cooled compression cost is high, between 2.2 and 3.36 €/kg. Having no compression on the distribution site (case c) is a very large advantage.

6.5.5.2 High-Pressure Buffer

Using higher pressure storage containers induces also a beneficial effect on the necessary volume for high-pressure buffers in the distribution station. However, this cost remains low, being between 0 and 0.26 €/kg.

6.5.5.3 Transportable Storage Containers

Even if the transportable storage containers might rather be used on a rental basis, investment costs and specific costs are estimated (costs without margin). The calculations have shown that the best is having storage units with a capacity of about 1 day of distribution (thus, here 20 kg).

(a) in current practice, 20 MPa storage containers consist of bundles with 12 50 L steel bottles for an overall mass of 1010 kg (0.9% of hydrogen content only).
(b) 30 MPa composite storage containers would be made from 2 bottles of 350 L containing 14.7 kg H_2 for a mass of 480 kg (3.2% hydrogen content).
(c) 52.5 MPa composite storage containers will be made of 2 bottles of 300 L containing 19.8 kg H_2 for a mass of 660 kg (3.0% hydrogen content).

These scenarios take the following into account:

- v_{sto}, the residual hydrogen returned to the production unit when a storage container is considered as empty,
- a minimum net autonomy of 2 days on the distribution site,
- a container number at least equal to the stage number (4 for b and c),
- a rotation every 2 or 3 days for the delivery of the bundles or containers,
- at least 1 container left on the production site for being filled.

This gives the total minimum number of containers, the overall autonomy, and the investment cost for the storage. The autonomy is then between 6.1 and 8.6 days. The absence of a compressor induces a high residual pressure in the returned containers and increases by 1 unit the number of necessary containers for 35 MPa distribution. With 52.5 MPa storage containers, due to the larger H_2 mass of the containers, the autonomy of the station exceeds 3 days. Thanks to their long lifetime, the depreciation of the storage investment cost is taken over 20 years, together with a 1.5% annual maintenance cost. Finally, the specific storage cost remains high, from 0.63 to 1.86 €/kg, but the increase for cases b and c with respect to case a is lower than the savings on the specific compression cost.

6.5.5.4 Transportation Material

The transportation material consists of a tractor and a flatbed trailer equipped with a handling crane; the calculation model shows:

(a) 5 bundles have to be delivered every 2 days to each of the 5 stations; the total mass is >25 tons and would necessitate a 38 t tractor and trailer with a high investment and a specific cost of 0.55 €/kg (including maintenance cost).

(b) 3 containers have to be delivered every 2 days to each HRS; the load is only 7.2 t and will require a lighter tractor and trailer, with a specific cost divided by 2, 0.26 €/kg

(c) the station autonomy is larger than 3 days and the supply of 2 or 3 stations every 3 days is planned, with the same material as for case b. The trailer load will be 8 t for 35 MPa distribution or 6 t for 70 MPa and with specific cost of the same order.

The round-trip delivery for 3 or 5 stations is 6 or 9 h long for 200 or 300 km, as the distance between stations is assumed to be 50 km, and with 30 min for loading and unloading in each place. The total mileage is 54,000 km/year for cases a and b, and 40,500 km/year for case c, thus the 3-day delivery period gives an advantage. The diesel consumption (at 1.04 €/L, VAT excluded) for transportation is highly affected by the mass of the hauler. It is 2.5 times higher for case a than for case b, and by the total distance, case c is even 20% and 35% less than b. Thus, the light composite containers reduce drastically the specific consumption and CO_2 emission to an acceptable level of 0.36 to 0.56 t_{CO2}/t_{H2}, instead of 1.46 t_{CO2}/t_{H2} for case a!

At this stage, it must be noticed that tractor and trailer are not used at full charge. They could make at least 3 times as many deliveries, decreasing the investment specific cost by a factor of 3 if this material were used in common for 3 production units.

6.5.5.5 Labor Cost

In all three cases, the deliveries can be made with one full time equivalent worker (1640 h/year) for a cost estimated to be 36 k€/year, which gives a high specific cost of 0.99 €/kg H2.

Table 6.14 also shows the premium costs of the 70 MPa distribution option with respect to the basic 35 MPa distribution, which is high at 0.74 €/kg with 30 MPa containers and 2.39 €/kg with 52.5 MPa! The availability of very-high-pressure transportable containers (e.g., 105 MPa) would reduce this gap for 70 MPa dispensing.

The cost for compression, storage, and transportation of hydrogen, for the purpose of the distribution of small quantities, was known to be high. Finally, this model confirms and quantifies these costs with details. It appears that the use of composite light bottle containers adapted to the distribution unit capacity

TABLE 6.14 Effect of Transportable Storage Choice on the Detailed Characteristics and Costs for Small 20 kg/Day HRSs Supplied by a 100 kg/Day Production Unit (Distance 50 km)

Refueling Stations: Number and Capacity (kg/Day)	5 HRSs of 20 kg/day Supplied From 1 Production Unit at 50 km					
Storage: case, type, pressure (MPa)	a, Steel, 20		b, Composite, 30		c, Composite, 52.5	
Distribution pressure (MPa)	35	70	35	70	35	70
Buffer pressure (MPa)	45	90	45	52.5 and 90	None	52.5 and 90
Fraction of compressed hydrogen (%)	100	100	35.8	63.9	0	41.2
Compressor investment cost (k€)	104	111	76	97	0	85
Compressor nominal electric power (kW_{el})	4.75	6.25	1.9	4.2	0	2.8
Reduction factor for progressive storage emptying	0.50	0.59	0.49	0.57	0	0.46
Electric consumption for cooled compression (MWh/an)	13.7	21.2	6.2	11.9	0	7.4
Electricity cost (k€/an)	1.1	1.7	0.5	0.9	0	0.6
Specific consumption for cooled compression (kWh/kg_{H2})	1.88	2.9	0.85	1.62	0	1.01
Specific consumption for cooled compression ($\%LHV_{H2}$)	5.6	8.7	2.5	4.9	0	3.0
Specific GHG emission (t_{CO2}/t_{H2})	0.11	0.17	0.05	0.10	0	0.06
Global cost for compression and cooling (€/kg_{H2})	3.07	3.36	2.21	2.86	0	2.48
High pressure buffer volume (L)	750	450	270	210+150	0	60+150
Buffer investment costs (k€)	14.5	15	6.6	11.6	0	8.0
Buffer specific cost (€/kg_{H2})	0.28	0.29	0.13	0.22	0	0.15
Unit storage hydrogen content (kg)	9.0		14.7		19.8	
Number of storages on distribution site	6		5		5	5

TABLE 6.14 Effect of Transportable Storage Choice on the Detailed Characteristics and Costs for Small 20 kg/Day HRSs Supplied by a 100 kg/Day Production Unit (Distance 50 km)—cont'd

Refueling Stations: Number and Capacity (kg/Day)	5 HRSs of 20 kg/day Supplied From 1 Production Unit at 50 km			
Number of storages in transit	5	3	3	2
Total number of storages	15	9	10	9
Overall autonomy (days)	6.1	6.2	8.2	8.6
Investment cost of storages (k€)	71	123	209	188
Storage specific cost (€/kg_{H2})	0.63	1.10	1.86	1.67
Mass of containers in transit (t)	5*5.05	5*1.44	3*2.65	2*2.65
Mass of tractor and trailer (t)	38	12	13	11
Equipment specific cost (€/kg_{H2})	0.55	0.26	0.28	0.23
Periodicity of deliveries (days)	2	2	3	3
Total annual mileage (km)	54,000	54,000	40,500	
Transport Diesel energy (MWh/yr)	192	76	61	49
Specific transport energy (kWh/kg_{H2})	5.25	2.07	1.66	1.34
Specific transport energy (% LHV_{H2})	15.7	6.2	5	4
Specific GHG emission (t_{CO2}/t_{H2})	1.42	0.56	0.45	0.36
Diesel specific cost (€/kg_{H2})	0.56	0.22	0.18	0.14
Labor cost: equivalent full time	1.0			
Specific labor cost (€/kg_{H2})	0.99			

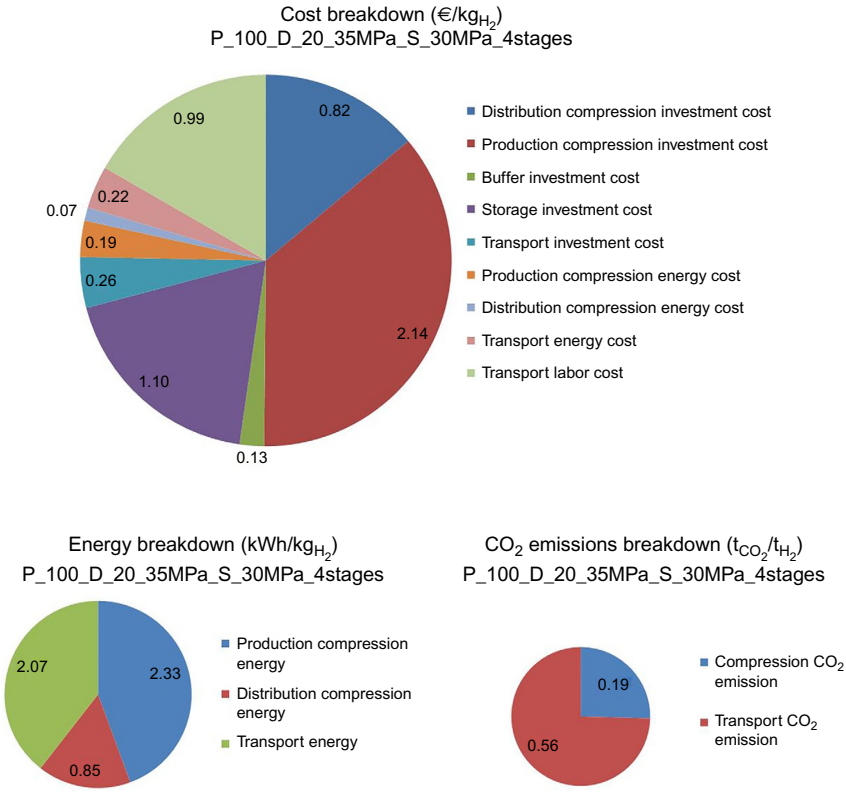

FIG. 6.11 Breakdown of cost, spent energy, and CO_2 emissions related to compression, storage, and transportation steps for a 20 kg/day 35 MPa refueling station supplied with 30 MPa hydrogen storage containers from a production unit at a distance of 50 km.

and a good distribution command-and-control strategy allow a significant decrease of this cost.

Moreover, one must keep in mind that these calculations have been made with the assumption that all refueling stations and production units are working at nominal load. A partial load would even increase the final specific cost. On the other hand, maximum load is twice the nominal load and working in between nominal and maximum load would decrease this cost.

The next section will show how the cost is drastically reduced for larger production units (200 and 400 kg/day) and larger HRSs (80 and 200 kg/day). These sizes are suitable for early hydrogen market deployment. For a mature market, HRSs of 400, 1000 kg/day, or even larger are considered, but it is probable that small capacity HRSs (80 and even 20 kg/day) will last and even expand in remote locations with low population densities.

Finally, the diagram of Fig. 6.11 illustrates the breakdown of cost, spent energy, and CO_2 emissions for this case, p_100_d_20, with 35 MPa distribution

and 4-stage 30 MPa storage units. The investment payback represents a very large part of the global cost, 75% with a large contribution from the compressors, especially on a distribution site. The suppression of a distribution compressor thanks to the use of 52.5 MPa storage containers is a great advantage!

6.5.6 Estimation of Global Costs, Effect of Capacity and Stage Number

6.5.6.1 Comparison of Reference Case 20 MPa Steel Tubes and 30 MPa Composite Containers

Fig. 6.12 shows a comprehensive view of the global cost for compression, storage, and transport in the reference case (20 MPa steel tubes) in blue, and in cases of 30 MPa light transportable composite containers in green. The same methodology and assumptions as in the previous section are used. The different considered cases show the effect of the size or capacity of the units:

(a) Case p_100_d_20 (as in previous section): one 100 kg/day production unit supplying five 20 kg/day refueling stations,
(b) Case p_200_d_80: one 200 kg/day production unit supplying 80 kg/day refueling stations,
(c) Case p_400_d_80: one 400 kg/day production unit supplying 80 kg/day refueling stations,
(d) Case p_400_d_200: one 400 kg/day production unit supplying 200 kg/day refueling stations.

Results are given for 1, 2, 3, or 4 containers on the distribution site so that the effect of the number of stages can be seen. Despite the high investment cost of the composite containers, when amortized over 20 years, and provided their size is adapted to the distribution capacity, it appears clearly that:

- The composite solution is always better than the steel tube solution: with only 1 stage, the gain varies from *15% to 4.6%* according to the case (from 61 to 13 c€/kg H_2).
- Increasing the number of stages from 1 to 4 is beneficial to the global cost. The benefit is very high for small 30 MPa refueling stations and decreases with capacity and distribution pressure: at 35 MPa *12%* for p_100_d_20 and *9%* for p_400_d_200; at 70 MPa *5.5%* for p_100_d_20 and *4%* for p_400_d_200.
- The effect of capacity is large: the cost of p_400_d_200 is *2.31* €/kg_{H2}, a *60%* reduction of the cost of p_100_d_20, 5.91 €/kg_{H2}.
- The extra cost for the 70-MPa option is higher for small capacities: 76 c€ (12.5%) for p_100_d_20 and 25 c€ (10.5%) for p_400_d_200.

Concerning the energy spent, the gain of the composite solution is also clear: −37% for p_100_d_20 at 5.67 kWh/kg_{H2}, −32% for p_400_d_200 at

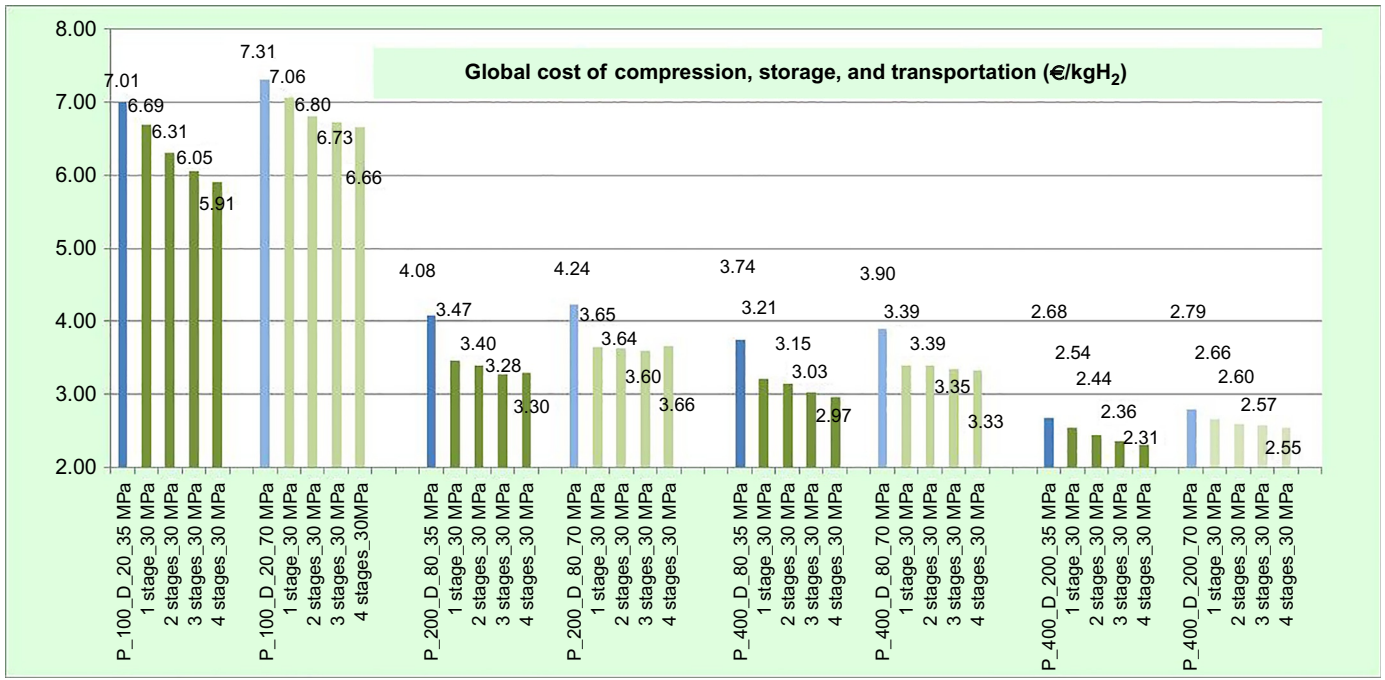

FIG. 6.12 Variation of global cost for compression, storage and transportation with the size of the units and the type of storage : reference steel 20 MPa (the *blue* and first bar of each series of 5) or composite 30 MPa with 1 to 4 stages (the 4 *green* following bars of each series of 5); 35 MPa distribution in *dark blue* or *green* (*dark grey* in print version) and 70 MPa distribution in *light blue* or *green* (*light grey* in print version).

3.52 kWh/kg $_{H2}$. Then, increasing the number of stages generates extra gains of −7.5% for p_100_d_20 and p_400_d_200. The 70-MPa refueling option costs 15 to 18% more energy than the 35-MPa option. The decay with the size is large: −35% from *5.25 kWh/kg$_{H2}$* for p_100_d_20 to *3.26 kWh/kg$_{H2}$* for p_400_d_200 (Fig. 6.13).

Concerning the CO_2 emissions, the results show similar trends. The large decrease for the reference steel storage between p_100_d_20 and p_200_d_80 is explained by the shift from bottle bundles to tube trailers with higher specific hydrogen content, inducing lower fuel consumption for transportation. The size effect reduces CO_2 emissions by 59% from *0.75* t_{CO2}/t_{H2} for p_100_d_20 to *0.31* t_{CO2}/t_{H2} for p_400_d_200 (Fig. 6.14).

6.5.6.2 Comparison Between 30-MPa and 52.5-MPa Composite Storage Containers

In Fig. 6.15, the best results for 30-MPa containers (with 4 stages) are compared to the results for 52.5-MPa containers with 1, 2, 3, and 4 stages for the same 4 cases as in the previous section in order to show the influence of increasing the pressure and the number of stages.

Of course, for 1-stage 35-MPa distribution without a compressor, because of the high level of hydrogen returned to production, 52.5-MPa storage generates a higher cost, but adding stages improves the results and finally generates appreciable savings with respect to the 30-MPa storage: *−29%*, i.e., −1.70 €/kg at 4.21 €/kg for p_100_d_20 and *−4%*, that is, −9 c€/kg at 2.22 €/kg for p_400_d_200.

For 70-MPa 80-kg/day distribution, the best costs are obtained with 3 stages and are very close (within 1% or 2%) of those obtained with 30-MPa storage; better for 200 kg/day production units and slightly higher for 400 kg/day production units.

Concerning the spent energy (Fig. 6.16), the best score is always obtained for four stages, with good improvements for p_100_d_20 at 35 MPa: −0.6 kWh/kg at 4.65 kWh/kg *(−13%)*, as at 70 MPa: −0.68 kWh/kg at 5.35 kWh/kg. At higher capacities, the advantages of the 52.5-MPa storage containers are less: the energy for their transportation is nearly unchanged and the compression energy saving at the distribution is nearly compensated by the extra compression energy at production. A specific energy as low as *3.11 kWh/kgH_2* can be reached.

For CO_2 emissions, the trends are the same and emissions as low as *0.29* t_{CO2}/t_{H2} can be reached (Fig. 6.17).

6.6 CONCLUSION

A methodology has been detailed to simply specify the components and evaluate the cost, the energy consumption, and the CO_2 emissions of the compression, storage, and transportation steps for hydrogen distribution. A numerical

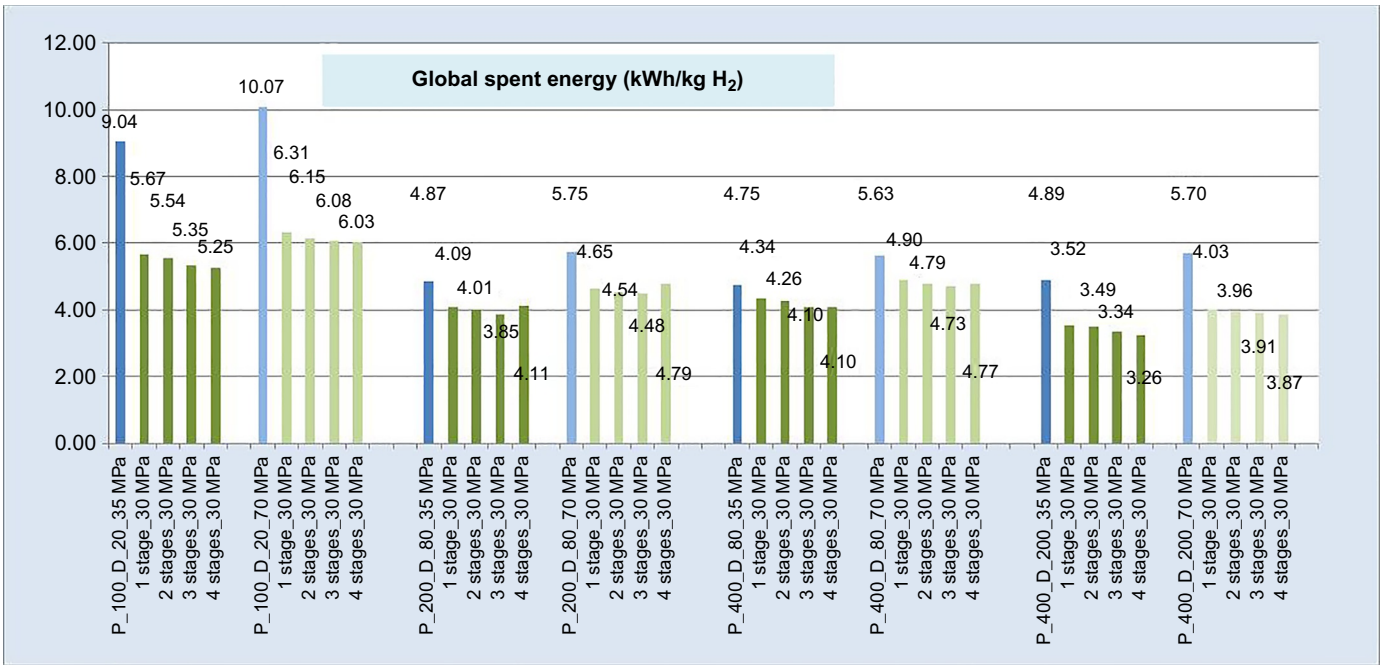

FIG. 6.13 Variation of global energy spent for compression, storage and transportation with the size of the units and the type of storage : reference steel 20 MPa (the *blue* and first bar of each series of 5) or composite 30 MPa with 1 to 4 stages (the 4 *green* following bars of each series of 5); 35 MPa distribution in *dark blue* or *green* (*dark grey* in print version) and 70 MPa distribution in *light blue* or *green* (*light grey* in print version).

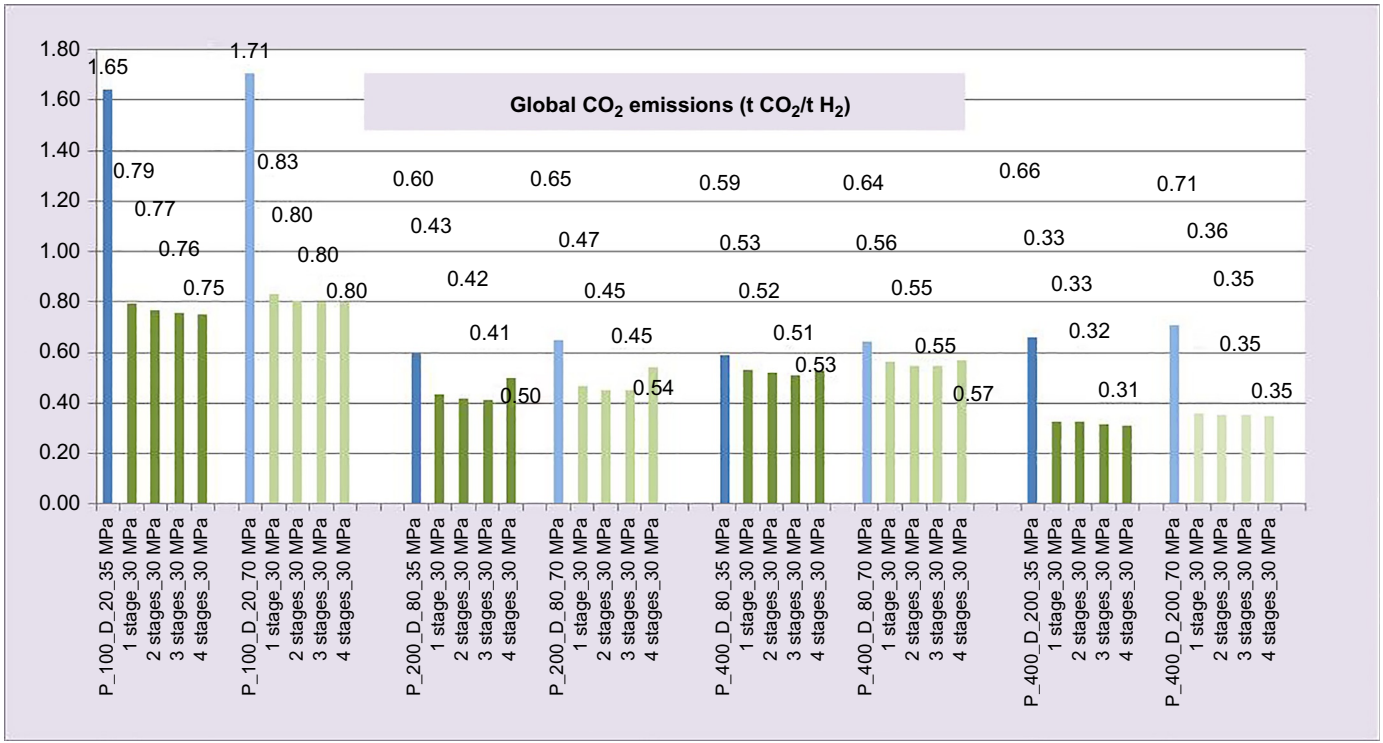

FIG. 6.14 Variation of the CO_2 emissions for compression, storage and transportation with the size of the units and the type of storage : reference steel 20 MPa (the *blue* and first bar of each series of 5) or composite 30 MPa with 1 to 4 stages (the 4 *green* following bars of each series of 5); 35 MPa distribution in *dark blue* or *green* (*dark grey* in print version) and 70 MPa distribution in *light blue* or *green* (*light grey* in print version).

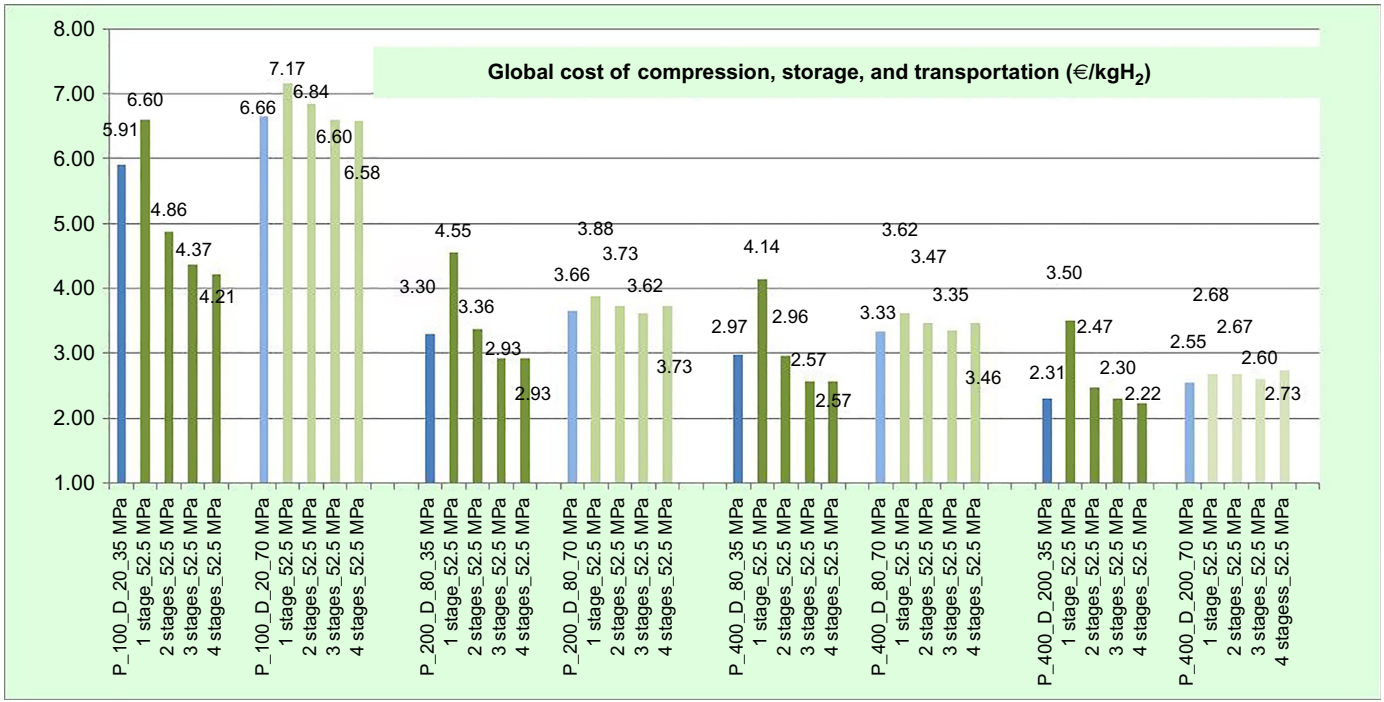

FIG. 6.15 Variation of global cost for compression, storage and transportation with the size of the units and the type of storage : reference steel 20 MPa (the *blue* and first bar of each series of 5) or composite 30 MPa with 1 to 4 stages (the 4 *green* following bars of each series of 5); 35 MPa distribution in *dark blue* or *green* (*dark grey* in print version) and 70 MPa distribution in *light blue* or *green* (*light grey* in print version).

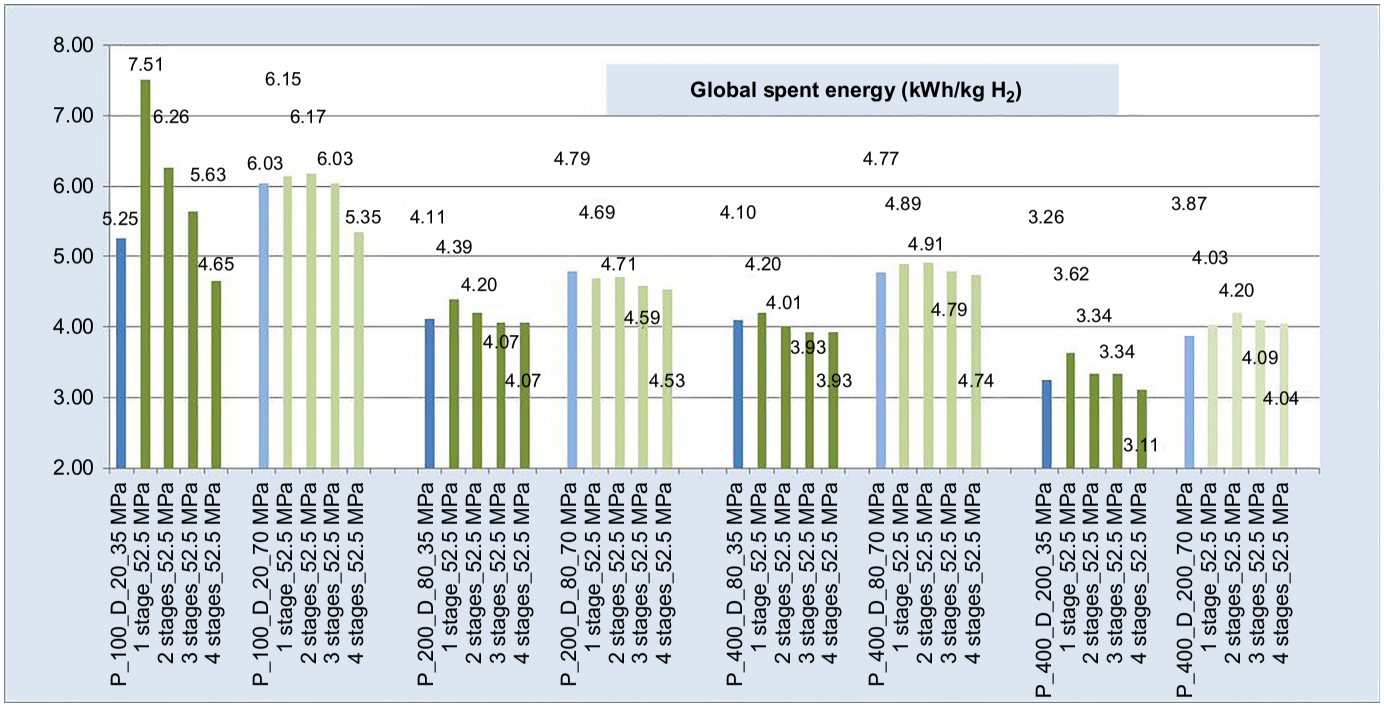

FIG. 6.16 Variation of global energy spent for compression, storage and transportation with the size of the units and the type of storage : reference steel 20 MPa (the blue and first bar of each series of 5) or composite 30 MPa with 1 to 4 stages (the 4 *green* following bars of each series of 5); 35 MPa distribution in *dark blue* or *green* (*dark grey* in print version) and 70 MPa distribution in *light blue* or *green* (*light grey* in print version).

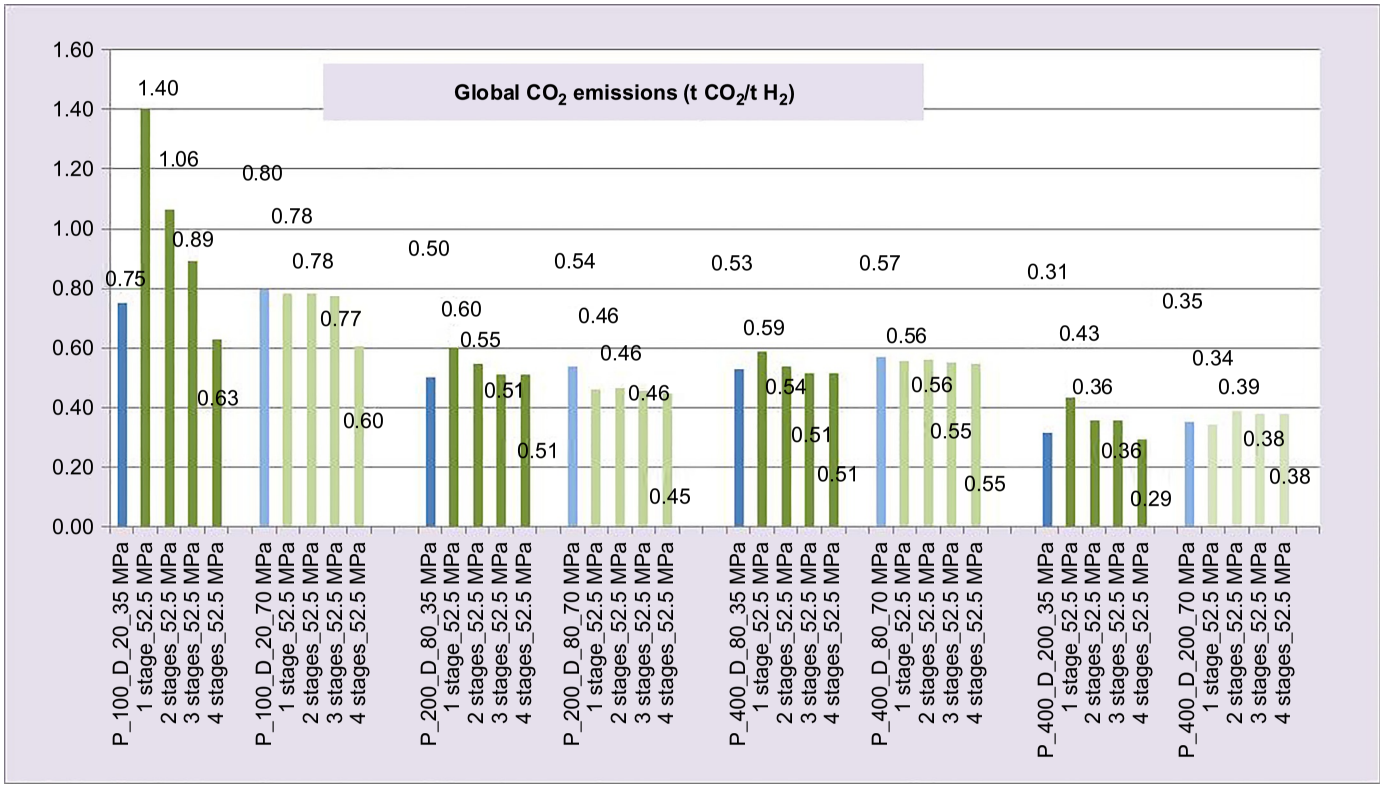

FIG. 6.17 Variation of the CO_2 emissions for compression, storage and transportation with the size of the units and the type of storage : reference steel 20 MPa (the *blue* and first bar of each series of 5) or composite 30 MPa with 1 to 4 stages (the 4 *green* following bars of each series of 5); 35 MPa distribution in *dark blue* or *green* (*dark grey* in print version) and 70 MPa distribution in *light blue* or *green* (*light grey* in print version).

tool has been developed on this basis. Results have been shown, together with the associated hypotheses, in some cases corresponding to small distribution units relevant to the early hydrogen market of the current and next years. The complete set of equations has been written to form a comprehensive model, which can be further used in other conditions or with other hypotheses by the reader.

Among the hypotheses of the model, the value of v_{tank}, the fraction of residual hydrogen in the tank as a vehicle comes to the refueling station, is a sensitive piece of data. The value used (2 MPa) can be considered low, thus inducing optimistic results. On the other hand, considering a load equal to the nominal load for the HRS is optimistic at the launch of the station, but as the maximum load equals twice the nominal load, with the further development of hydrogen vehicle fleets, this assumption will become pessimistic! And finally, it can be correct over the lifetime of the HRS.

For the case of *hydrogen distribution on the site of its production*, the energy need for cooled compression is evaluated at *3.50 or 4.4 kWh/kg$_{H2}$* at *35 or 70 MPa, in the reference case*, corresponding to current practice. The study has shown that this energy need can be *reduced by >25%* when judiciously using *4 or 5 stages* of buffers organized in a pressure cascade for the filling of the tanks. Whereas these staged pressure buffers have higher volumes and costs than the usual very-high-pressure buffer (VHPB), the extra capital cost is acceptable and the energy saving results in an acceptable payback time of *4.5–5.5 years*.

In the case in which a production unit supplies hydrogen to *several distant distribution units*, energy for transportation by truck and for recompression on the distribution site must be added. The offsite distribution current practice considers the transportation of 20 MPa hydrogen steel bottle bundles or tube trailers and the recompression of all the hydrogen to the VHPB.

To lower the energy spending, small containers of 30 MPa light composite bottles can be used. Trucks can then transport loads with a three times larger hydrogen content. These containers can be used as well in the place of intermediate pressure buffers on the distribution site for prefilling of the tanks; just a small VHPB has to be kept and only a small part of the hydrogen has to be compressed to this VHPB.

The study shows that, even if the investment in composite bottle containers is high, the resulting overall cost is always lower. The use of up to 4 containers on the distribution site generates a global cost reduction of *27%–14%* for a distribution at 35 MPa, decreasing with the capacity (and 20.5–8.5% at 70 MPa). The energy savings are high, in a range of *42–14%* when shifting from steel 20 MPa to composite 30 MPa according to the different studied cases.

When higher pressure composite containers are available (52.5 MPa), then a compressor and VHPB are useless for distribution at 35 MPa and this results in *significant supplementary reductions* of investment cost, global cost *(−29%)*, and energy needs *(−13%)*, especially for small capacities, while for a

distribution at 70 MPa, 52.5-MPa containers give very similar results to 30-MPa containers.

The overall energy expenditure can be *lower than 3.1 kWh/kg$_{H2}$* for a 35 MPa distribution (*4.04 kWh/kg$_{H2}$* for 70 MPa) and the CO_2 emissions lower than *0.30 t$_{CO2}$/t$_{H2}$* for a 35 MPa distribution (*0.38 t$_{CO2}$/t$_{H2}$* for 70 MPa).

These small, light, composite 52.5 MPa hydrogen containers generate interesting savings in operational costs and also drastic simplification for 35-MPa distributions. Thus, 20, 80, and 200 kg_{H2} containers are currently being developed in the framework of the VABHYOGAZ3 project by ALBHYON office of HERA, the company leader of the project. They will be certified for road transportation and implemented on the test sites of the project, and they will also be available as commercial products as a result of the project. Also being developed is the 35 MPa distribution unit adapted to these 52.5 MPa containers. It is very simple, it does not have any compressor nor any HP buffer, its cost will be low and it will make hydrogen available and affordable in many places. 70-MPa distribution units adapted to these 52.5-MPa container cascades will be another product resulting from the project, developed by ALBHYON, as they have the know-how for designing, manufacturing (with their supplier network), certifying, and implementing these solutions on those sites interested in small- or medium-scale hydrogen production and distribution.

Finally, it should be recalled that all costs presented in this paper are current costs as the results are to be applied now or in the next few years. No reduction for large quantity production is taken into account yet. However, these reductions will undoubtedly occur, as normally occurs in any domain when a new product progressively acquires a growing maturity and is produced in larger and larger quantities. This is known as "the learning curve" In a contiguous field of hydrogen energy, Staffell and Green (2013) shows how the prices of domestic fuel cells for combined heat and power generation have been decreasing in the past decade; it also recalls that this phenomenon has been noticed for other products from the energy sector, with a 15%–20% decay in the cost of a system noticed each time the produced quantity doubles. So, there is great hope that the costs announced in this paper are going to decrease significantly in the next decade.

APPENDIX 1 WORK FOR THE PROGRESSIVE FILLING OF A STORAGE CONTAINER

In some cases, the compressor does not always work at its nominal pressure ratio, for example when a trailer or a storage container comes back to the production site nearly empty, with a pressure $p_{sto,f}$ to be refilled up to the pressure $p_{sto,0}$. While the inlet pressure of the compressor is constant at p_{prod}, the filling begins with a low pressure ratio, $r_{p,f}$, and this pressure ratio increases progressively up to $r_{p,0}$ as the compressor fills the storage container. Thus the compressor starts at low power and ends at its nominal power.

$$r_{p,f} = {}^{p_{sto,f}}/_{p_{prod}} \quad r_{p,0} = {}^{p_{sto,0}}/_{p_{prod}}$$

It is easy to calculate the energy need along this progressive filling in the case of a perfect gas and of an isothermal compression.

For an isothermal compression of an increment of mass dm from p_{prod} up to p_{sto}, the useful energy need is:

$$dW_{filling} = k * dm * \ln\left({}^{p_{sto}}/_{p_{prod}}\right) \quad \text{with} \quad k = \frac{R}{M} * T_0$$

The total energy need to fill the storage from $p_{sto,f}$ to $p_{sto,0}$ from a production unit at p_{prod} is equal to the integral:

$$W_{filling} = \int_{p_{sto}=p_{sto,f}}^{p_{sto,0}} k * dm * \ln\left({}^{p_{sto}}/_{p_{prod}}\right)$$

The pressure in the storage container in linked to the mass of gas present in the tank; for a perfect gas, an increment of mass dm induces an isothermal increment of pressure dp linked to the final pressure $p_{sto,0}$ and final mass $m_{sto,0}$ in the storage:

$$dm \Big/ {}_{m_{sto,0}} = {}^{+dp}/_{p_{sto,0}}$$

$$W_{filling} = +k * {}^{m_{sto,0}}/_{p_{sto,0}} * \int_{p=p_{sto,f}}^{p_{sto,0}} \ln\left({}^{p_{sto}}/_{p_{prod}}\right) * dp$$

Introducing the new variable:

$$r_p = {}^{p_{sto}}/_{p_{prod}}$$

$$W_{filling} = +k * m_{sto,0} * {}^{p_{prod}}/_{p_{sto,0}} * \int_{r_p=r_{p,f}=\frac{p_{sto,f}}{p_{prod}}}^{r_{p0}=\frac{p_{sto,0}}{p_{prod}}} \ln\left(r_p\right) * dr_p$$

The primitive function of $f(x) = \ln(x)$ is $F(x) = x^*(\ln(x) - 1)$, thus it comes:

$$W_{filling} = +k * m_{sto,0}/r_{p,0} * \left[r_p\left(\ln\left(r_p\right) - 1\right)\right]_{r_{pf}}^{r_{p,0}}$$

$$W_{filling} = k * \frac{m_{sto,0}}{r_{p,0}} * \left\{r_{p,0} * \left(\ln\left(r_{p,0}\right) - 1\right) - r_{p,f} * \left(\ln\left(r_{p,f}\right) - 1\right)\right\}$$

TABLE A.1 Comparison of Progressive Filling of Storage (Increasing Pressure Ratio) With Constant Pressure Ratio Compression, Isothermal, Perfect Gas, $p_{prod} = 1.5$ MPa, Storage Initial Pressure $p_{sto,f} = 2$ MPa

Storage Pressure p_{sto} (MPa)	20	30	52.5
Initial pressure ratio $r_{p,\,f}$	1.33	1.33	1.33
Final pressure ratio $\boldsymbol{r_{p,0}}$	13.3	20	35
Energy for progressive isothermal filling from $r_{p,\,f}$ to $r_{p,\,0}$	1.85*k	2.19*k	2.68*k
Energy for isothermal filling at constant $r_{p,\,0}$	2.59*k	3.00*k	3.56*k
Reduction factor for progressive filling	0.713	0.731	0.755

During this filling, the mass of the storage increases from $m_{sto,0} * v_{sto}$ to $m_{sto,0}$ with:

$$v_{sto} = {}^{p_{sto,f}}\!/_{p_{sto,0}} = {}^{r_{p,f}}\!/_{r_{p,0}}$$

Thus, the transferred mass is $m_{sto,0} * (1 - v_{sto})$ and finally the energy need per unit transferred mass is:

$${}^{W_{filling}}\!/_{m_{transf}} = k * \frac{1}{r_{p,0} * (1 - v_{sto})} * \left\{ r_{p,0} * \left(\ln\left(r_{p,0}\right) - 1 \right) - r_{p,f} * \left(\ln\left(r_{p,f}\right) - 1 \right) \right\}$$

Otherwise, this energy for filling a storage container with an increasing pressure ratio from $r_{p,\,f}$ to $r_{p,0}$ can be compared with the energy for a perfect gas isothermal compression of constant pressure ratio $r_{p,\,0}$, which is Eq. (6.3):

$${}^{W_{isothermal,\,perfect}}\!/_{m} = k * \ln\left(r_{p,0}\right)$$

Some numerical values are given in the Table A.1, which are used in Section 6.5:

It can be seen that the filling of a storage container with a progressively increasing pressure costs 25–30% less than filling at a constant pressure.

APPENDIX 2 WORK FOR EMPTYING A STORAGE CONTAINER TO A HIGHER-PRESSURE BUFFER

Sometimes, the opposite case happens and the compressor has always the same outlet pressure, but the inlet pressure varies and the compressor does not always work at its nominal pressure ratio. This happens, for example, when a trailer or a storage container is used to fill the buffer of a refueling station. While the pressure buffer is kept constant by the compressor at p_{buff}, at the beginning the trailer

or the storage is at a high pressure, $p_{sto,0}$, and the buffer filling begins with a low pressure ratio $r_{p,0}$; then the pressure ratio increases progressively up to $r_{p,f}$ as the compressor empties the storage container down to $p_{sto,f}$. Again, the compressor starts at low power and ends at its nominal power. Again, it is easy to integrate the energy needs along this progressive emptying in the case of a perfect gas and of an isothermal compression.

The total energy need for an isothermal compression when emptying the storage container from $p_{sto,0}$ to $p_{sto,f}$ while keeping the buffer at p_{buff} is equal to the integral:

$$W_{emptying} = \int_{p_{sto}=p_{sto,0}}^{p_{sto,f}} k * dm * \ln\left({}^{p_{buff}}\!/_{p_{sto}}\right)$$

The pressure in the storage container is linked to the mass of gas present in the container; for a perfect gas:

$${}^{dm}\!/_{m_{sto,0}} = -{}^{dp}\!/_{p_{sto,0}}$$

$$W_{emptying} = -k * {}^{m_{sto,0}}\!/_{p_{sto,0}} * \int_{p=p_{sto,0}}^{p_{sto,f}} \ln\left({}^{p_{buff}}\!/_{p_{sto}}\right) * dp$$

Introducing the new variable:

$$x = {}^{p_{sto}}\!/_{p_{buff}} = {}^{1}\!/_{r_p}$$

$$W_{emptying} = +k * m_{sto,0} * {}^{p_{buff}}\!/_{p_{sto,0}} * \int_{x=x_0=\frac{p_{sto,0}}{p_{buff}}}^{x_f=\frac{p_{sto,f}}{p_{buff}}} \ln(x) * dx$$

$$W_{emptying} = +\ k * m_{sto,0} * r_{p,0} * \left[x(\ln(x) - 1)\right]_{x_0=\frac{1}{r_{p,0}}}^{x_f={}^{1}\!/_{r_{p,f}}}$$

$$W_{emptying} = -k * \frac{m_{sto,0}}{r_{p,f}} * \left\{r_{p,0} * \left(\ln\left(r_{p,f}\right) + 1\right) - r_{p,f} * \left(\ln\left(r_{p,0}\right) + 1\right)\right\}$$

During this emptying, the mass of the storage decreases from $m_{sto,0}$ to $m_{sto,0} * v_{sto}$. So, the transferred mass is $m_{sto,0} * (1 - v_{sto})$ and finally the energy need per unit transferred mass is:

$${}^{W_{emptying}}\!/_{m_{transf}} = -k * \frac{1}{r_{p,f} * (1 - v_{sto})} * \left\{r_{p,0} * \left(\ln\left(r_{p,f}\right) + 1\right) - r_{p,f} * \left(\ln\left(r_{p,0}\right) + 1\right)\right\}$$

TABLE A.2 Comparison of Progressive Emptying of Storage to Fill a Buffer (Increasing Pressure Ratio) With Constant Pressure Ratio Compression, Isothermal, Perfect Gas, p_{buff} = 45 or 90 MPa, Storage Final Pressure $p_{sto,f}$ = 2 MPa

Buffer Pressure p_{buff} (MPa)	45		90		
Nominal storage pressure $p_{sto,0}$ (MPa)	20	30	20	30	52.5
Initial pressure ratio $r_{p,0}$	2.25	1.5	4.5	3	1.71
Final pressure ratio $r_{p,f}$	22.5	22.5	45	45	45
Energy for progressive isothermal emptying from $r_{p,0}$ to $r_{p,f}$	1.56*k	1.21*k	2.25*k	1.90*k	1.41*k
Energy for isothermal emptying at constant $r_{p,0}$: $\ln(r_{p,f})$	3.11*k	3.11*k	3.81*k	3.81*k	3.81*k
Reduction factor for progressive emptying	0.499	0.389	0.591	0.500	0,370

Otherwise, this energy for keeping the buffer at its pressure while emptying a storage container with an increasing pressure ratio from $r_{p,0}$ to $r_{p,f}$ can be compared to the energy for a perfect gas isothermal compression in constant pressure ratio $r_{p,f}$, which is Eq. (6.3).

Some numerical values are given in the Table A.2, which are used in Section 6.5.

It can be seen that emptying a storage container with a progressively increasing pressure ratio in order to keep a buffer at its nominal pressure costs 41%–63% less than using the constant high-pressure ratio.

At this stage it is interesting to compare the compression energies in the cases of onsite and distant distributions. For distribution on the production site, only one compression is needed, at a constant high-pressure ratio. For a distant distribution, there are two compressions, but at increasing pressure ratio, with lower energy demand, as shown in Table A.3.

The last line of Table A.3 shows that the intermediate step of storage for transportation does not induce any increase in the compression energy demand, *provided the gas is perfect and the compression isothermal*. This result could be intuited, as this calculation is related to *only the useful work*, with no losses in heating the gas. It will no longer be the same in real cases with hydrogen real gas, imperfectly cooled compressions, and efficiency losses in the compressors.

TABLE A.3 Comparison of the Energies for Compression: On Production Site Distribution Versus Off Production Site Distribution; Isothermal, Perfect Gas, $p_{prod} = 1.5$ MPa, Storage Initial Pressure $p_{sto,f} = 2$ MPa

	OnSite Dispensing (35 or 70 MPa)		*OffSite* Dispensing (35 or 70 MPa)				
Buffer pressure p_{buff} (MPa)	45	90	45		90		
Nominal storage pressure $p_{sto,0}$ (MPa)	Without		20	30	20	30	52.5
Compression energy on the production site	3.40*k	4.09*k	1.85*k	2.19*k	1.85*k	2.19*k	2.68*k
Compression energy for dispensing on the distribution site	Included	Included	1.56*k	1.21*k	2.25*k	1.90*k	1.41*k
Total compression energy	3.40*k	4.09*k	3.40*k	3.40*k	4.09*k	4.09*k	4.09*k

APPENDIX 3 SCENARIO FOR REFUELING WITH SEVERAL STORAGE UNITS AT A HIGHER INITIAL PRESSURE THAN THE TANKS TO BE FILLED

In a hydrogen refueling station supplied with transportable containers at a nominal pressure higher than the nominal pressure of the tanks to be filled (e.g., $p_{sto} = 52.5\,\text{MPa}$ for $p_{tank} = 35\,\text{MPa}$), there is no need for a compressor, nor for high-pressure buffers. But it is necessary to dispose of several storage containers and these will be returned to the production unit with some residual hydrogen pressure.

This appendix formulates the analytical equations to calculate this residual pressure as a function of the number of storage containers available at the station. The equations are written for a perfect gas: at any temperature, pressure and specific mass in the vessel are proportional. This formulation is based on *a scenario in which all vehicles arrive at the station with the same filling state of their tank and are all filled in the same way from a cascade of storage containers*.

Consider the case of four storage containers available at the station numbered 1, 2, 3 and 4.

Consider a first vehicle with a tank of nominal contained mass m_{tank} at nominal pressure p_{tank} arriving at the station with a residual hydrogen pressure and mass $v_{tank,0}$:

$$p_{tank,0} = v_{tank,0} * p_{tank} \quad m_{tank,0} = v_{tank,0} * m_{tank}$$

Consider this vehicle has been filled to a fraction, $v_{tank,3}$, of its nominal mass from storage containers 4, 3, and 2. It contains a mass $v_{tank,3} * m_{tank}$. Then, the storage container 1 completes the filling with a mass $(1 - v_{tank,3}) * m_{tank}$ up to the pressure p_{tank}. The hydrogen mass of storage container 1, which was initially $m_{sto,0}$, decreases to $m_{sto,0} - (1 - v_{tank,3}) * m_{tank}$ while its pressure, initially $p_{sto,0}$, decreases down to

$$p_{sto,1} = p_{sto,0} * \left(1 - (1 - v_{tank,3})^{m_{tank}/m_{sto,0}}\right) = p_{sto,0} * (1 - (1 - v_{tank,3}) * a)$$

$$\text{with} \quad a = {}^{m_{tank}}/_{m_{sto,0}}$$

After having filled n such vehicles, the pressure and the mass in the storage container 1 are:

$$m_{sto,1} = m_{sto,0} * (1 - n * (1 - v_{tank,3}) * a) \quad p_{sto,1} = p_{sto,0} * (1 - n * (1 - v_{tank,3}) * a)$$

After N vehicles, storage container 1 pressure reaches its minimum value and is connected in the place of storage container 2:

$$m_{sto,1,\min} = m_{sto,2,0} = m_{sto,0} * (1 - N * a * (1 - v_{tank,3}))$$

$$p_{sto,1,\min} = p_{sto,2,0} = p_{sto,0} * (1 - N * a * (1 - v_{tank,3}))$$

Another new storage unit, at full pressure $p_{sto,0}$, replaces the unit 1; while the unit 2 replaces the unit 3 and unit 3 replaces the unit 4.

For the first vehicle, within the mass $v_{tank,3} * m_{tank}$, the contribution from the storage containers 4 and 3 has been $v_{tank,2} * m_{tank}$ and that of storage container 2 is $(v_{tank,3} - v_{tank,2}) * m_{tank.}$

In the same way, after N other vehicles have been filled, the pressure and mass in storage container 2 are:

$$m_{sto,2,\min} = m_{sto,3,0} = m_{sto,0} * (1 - N * a * (1 - v_{tank,2}))$$

$$p_{sto,2,\min} = p_{sto,3,0} = p_{sto,0} * (1 - N * a * (1 - v_{tank,2}))$$

At that moment, a new full storage container at $p_{sto,0}$ is connected in the place of storage container 1, while storage container 1 is connected in the place of storage container 2, storage container 2 takes the place of storage container 3, and storage container 3 takes the place of storage container 4.

For these vehicles, within the mass $v_{tank,2} * m_{tank}$, the contribution from storage container 4 has been $v_{tank,1} * m_{tank}$ and that of storage container 3 is $(v_{tank,2} - v_{tank,1}) * m_{tank}$.

In the same way, after N other vehicles have been filled, the pressure and mass in storage container 3 are:

$$m_{sto,3,\min} = m_{sto,4,0} = m_{sto,0} * (1 - N * a * (1 - v_{tank,1}))$$

$$p_{sto,3,\min} = p_{sto,4,0} = p_{sto,0} * (1 - N * a * (1 - v_{tank,1}))$$

At that moment the 3rd permutation takes place, a new full storage container at $p_{sto,0}$ is connected in the place of storage container 1 while storage container 1 is connected in the place of storage container 2, storage container 2 takes the place of storage container 3, and storage container 3 the place of storage container 4.

Within the mass $v_{tank,1} * m_{tank}$, the contribution of storage container 4 is $(v_{tank,1} - v_{tank,0}) * m_{tank}$ as the vehicle arrived with a residual mass $v_{tank,\ 0} * m_{tank}$.

A 4th series of N vehicles is being filled, the residual pressure and mass in storage container 4 are:

$$m_{sto,4,\min} = m_{sto,residu} = m_{sto,0} * (1 - N * a * (1 - v_{tank,0}))$$

$$p_{sto,4,\min} = p_{sto,residu} = p_{sto,0} * (1 - N * a * (1 - v_{tank,0}))$$

These are the mass and pressure at which the storage containers are considered empty and returned to the hydrogen production unit:

$$p_{sto,residu} = p_{sto,0} * v_{sto} \quad so \ (1 - v_{sto}) = N * a * (1 - v_{tank,0}))$$

$(1 - v_{sto})$ is the fraction of hydrogen of the storage that is effectively used. $4 * N$ is the number of vehicles that can be served with 4 stages of containers. d is introduced:

$$d = N * a = {}^{(1-v_{sto})} \Big/ {}_{(1-v_{tank,0})}$$

At this stage, it can be noticed that it is not necessary that all the vehicles have the same tank capacity and the same filling rate as they arrive at the station. The important quantity is the product $N * a$ or the sum of the a_i from which their average can be calculated and the average of their filling rate at their arrival to the station:

$$\overline{a} = \frac{1}{N} \sum a_i$$

$$\overline{v_{tank,0}} = \frac{1}{N} \sum v_{tank,0,\ i}$$

The values of the coefficients $v_{tank,1}$, $v_{tank,2}$,$v_{tank,3}$ are essential and they cannot be chosen, they must be calculated considering constraints on the storage. The storage pressure must be high enough to ensure the transfer from the storage container to the tank, even after the Nth vehicle. The overpressure Sp_{min} is introduced (Fig. A.1). Then the complete set of constraints to consider is:

$$p_{sto,1,0} = p_{sto,0}$$

$$p_{sto,1,\min} = p_{sto,2,0} = p_{sto,0} * (1 - d * (1 - v_{tank,3})) > p_{tank,4} * Sp_{min} = 1 * p_{tank} * Sp_{min}$$

$$p_{sto,2,\min} = p_{sto,3,0} = p_{sto,0} * \left(1 - d * \left(1 - v_{tank,2}\right)\right) > p_{tank,3} * Sp_{min} = v_{tank,3} * p_{tank} * Sp_{min}$$

$$p_{sto,3,\min} = p_{sto,4,0} = p_{sto,0} * \left(1 - d * \left(1 - v_{tank,1}\right)\right) > p_{tank,2} * Sp_{min} = v_{tank,2} * p_{tank} * Sp_{min}$$

$$p_{sto,4,\min} = p_{sto,0} * v_{sto} = p_{sto,0} * \left(1 - d * \left(1 - v_{tank,0}\right)\right) > p_{tank,1} * Sp_{min} = v_{tank,1} * p_{tank} * Sp_{min}$$

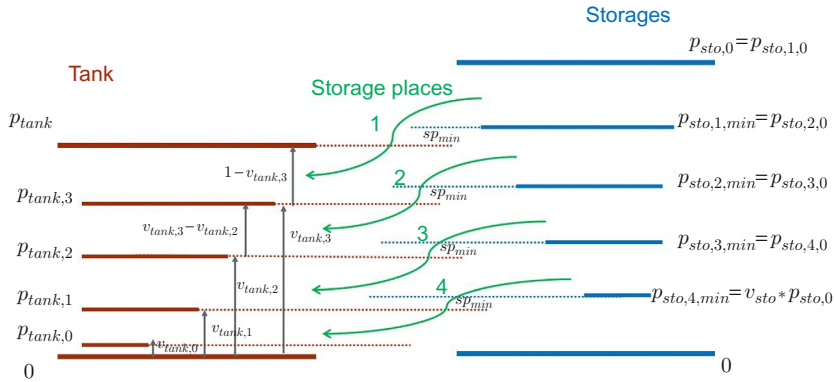

FIG. A.1 Schematic diagram for the filling of a tank from a cascade of storage containers.

When replacing the signs > by signs =, four equations are obtained, the solution of which allows calculating the minimum values of the four quantities $v_{tank,1}$,$v_{tank,2}$,$v_{tank,3}$, and $v_{sto,0}$. This means that the residual pressure with which storage containers are returned to the production unit cannot be chosen. It is imposed and highly sensitive to the quantity $v_{tank,0}$, the average filling rate at which the vehicles arrive at the station.

Another scenario may be considered for refueling. The quantity to transfer to the tank from a given storage container could be not maintained at the same level as the storage pressure decreases. It could be the maximum possible quantity transferable at any time. Then, the first vehicles of the series of the N vehicles would receive a higher contribution from the storage containers 4 and 3 and a lower contribution from the storage containers 2 and 1; but the opposite would happen for the last vehicles of the series; the contribution of storage containers 4 and 3 would be less as their pressure has decreased and storage containers 2 and 1 would have to complement with a larger contribution. Globally the equation for the definition of d shows that the same number of vehicles, $4*N$, could be served from the storage containers.

In the case in which only three storage containers are available at the station, the same series of equations can be used. Just do not calculate $v_{tank,3}$ and consider $v_{tank,3}=v_{tank,2}$ and $p_{sto,3,min}=p_{sto,4,min}$.

In the case in which only two storage containers are available at the station, the same series of equations can be used. Just do not calculate $v_{tank,\ 3}$ and $v_{tank,2}$ and consider: $v_{tank,3}=v_{tank,2}=v_{tank,1}$, $p_{sto,2,min}=p_{sto,3,min}=p_{sto,4,min}$.

APPENDIX 4 SCENARIO FOR REFUELING WITH A COMPRESSOR, A BUFFER AND SEVERAL STORAGE UNITS AT A LOWER INITIAL PRESSURE THAN THE TANKS TO BE FILLED

In a hydrogen refueling station supplied with transportable containers at a nominal pressure lower than the nominal pressure of the tanks to be filled, a compressor is mandatory and a very-high-pressure buffer as well (e.g., p_{sto} =30 MPa and p_{tank} =35 MPa with p_{buff} =45 MPa). This very-high-pressure buffer is filled by the compressor sucking hydrogen from one of the storage containers, and completes the filling of the tanks as the last stage of the cascade.

The analytical equations have been formulated for the compressor sucking from any storage stage; results have shown that the contribution of the compressor (the fraction of hydrogen to be compressed) is the lowest when the compressor sucks from the lowest pressure storage (as in Fig. A.2). Equations are shown in this case. The formulation is based on the same scenario as in Appendix 3 and the equations are very similar. The only differences are:

- The initial pressure of the 2nd storage (for the before last refueling stage) is equal to the nominal pressure of the full storage $p_{sto,0}$,
- 1 is substituted by $v_{tank,3}$ in the equations:

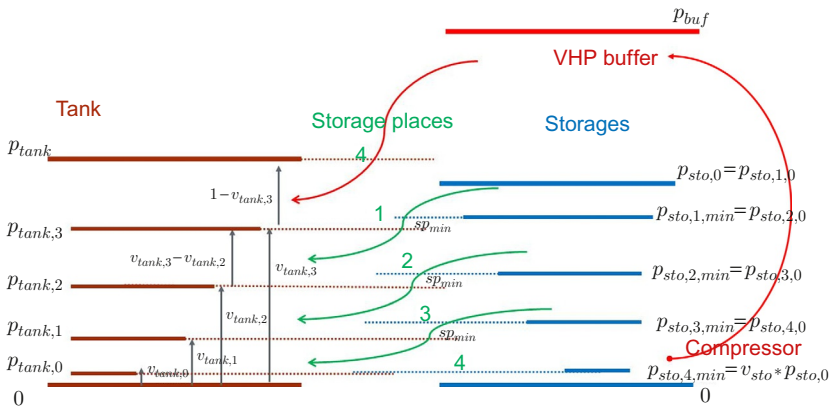

FIG. A.2 Schematic diagram for the filling of a tank from a cascade of storage containers, a compressor, and a very-high-pressure buffer.

$$p_{sto,2,0}=p_{sto,0}$$

$$p_{sto,2,\min}=p_{sto,3,0}=p_{sto,0}*\left(1-d*\left(v_{tank,3}-v_{tank,2}\right)\right)>p_{tank,3}*Sp_{min}=v_{tank,3}*p_{tank}*Sp_{min}$$

$$p_{sto,3,\min}=p_{sto,4,0}=p_{sto,0}*\left(1-d*\left(v_{tank,3}-v_{tank,1}\right)\right)>p_{tank,2}*Sp_{min}=v_{tank,2}*p_{tank}*Sp_{min}$$

$$p_{sto,4,\min}=p_{sto,1,0}=p_{sto,0}*\left(1-d*\left(v_{tank,3}-v_{tank,0}\right)\right)>p_{tank,1}*Sp_{min}=v_{tank,1}*p_{tank}*Sp_{min}$$

$p_{sto,1,min}=p_{sto,residu}=p_{sto,0}*v_{sto}$ without any constraint as this storage is feeding the compressor.

When replacing the signs $>$ by signs $=$, three equations are obtained the solution of which allows calculating the minimum values of the three quantities $v_{tank,1}$,$v_{tank,2}$, $v_{tank,3}$. The value of $v_{sto,0}$, giving the residual pressure of the storage containers when returned to the production unit, can be chosen. It allows calculating the pressure ratio of which the compressor must be capable. The value $(1-v_{tank,3})$ is the fraction of the hydrogen to be compressed (on a total of $(1-v_{tank,0})$).

ACKNOWLEDGMENT

This work is a part of the *VABHYOGAZ3* project supported by the French "Programme d'Investissements d'Avenir" under supervision of *ADEME*, the French Energy and Environment Agency. The project is conducted by *HERA France* office *ALBHYON*, in partnership with *TRIFYL, HP Systems, EMTA* (*VEOLIA* group) and the *IMT Mines-Albi RAPSODEE Research Center*. The VABHYOGAZ3 project considers hydrogen production from biogas with production units ranging from 100 to 800 kg/day to deliver hydrogen to several distribution units of 20–200 kg/day located within a distance <100 km from the production unit. The authors are grateful to the ADEME for its support to this project.

REFERENCES

Bourgeois, T., Ammouri, F., Weber, M., Knapik, C., 2015. Evaluating the temperature inside a tank during a filling with highly pressurized gas. Int. J. Hydrog. Energy 40, 11748–11755.

Bourgeois, T., Brachmann, T., Barth, F., Ammouri, F., Baraldi, D., Melideo, D., Acosta-Iborra, B., Zaepffel, D., Saury, D., Lemonnier, D., 2017. Optimization of hydrogen vehicle refuelling requirements. Int. J. Hydrog. Energy 1–21. https://doi.org/10.1016/j.ijhydene.2017.01.165.

Gardiner, M., July 2009. Energy Requirements for Hydrogen Gas Compression and Liquefaction as Related to Vehicle Storage Needs. U.S. Department of Energy Hydrogen and Fuel Cells Program Record No. 9013, http://www.hydrogen.energy.gov/pdfs/9013_energy_requirements_for_hydrogen_gas_compression.pdf.

Klell, M., Kindermann, H., Christian, J., 2007. Thermodynamics of gaseous and liquid hydrogen storage. In: Proceedings of IHEC 2007 the International Hydrogen Energy Congress and Exhibition, Istanbul, Turkey, 13–15 July. http://www.hycenta.tugraz.at/Image/Thermodynamics%20of%20gaseous%20and%20liquid%20hydrogen%20storage.pdf.

Lee, S., Kim, Y., Kim, S., Yoon, K., 2009. Temperature change of a type IV cylinder during hydrogen fueling process. In: Proceedings of the International Conference on Hydrogen Safety, Ajaccio. 2009.

Lei, Z., Yanlei, L., Jian, Y., Yongzhi, Z., Jinyang, Z., Haiyan, B., Xianxin, L., 2010. Numerical simulation of temperature rise within hydrogen vehicle cylinder during refueling. Int. J. Hydrog. Energy 35, 8092–8100. https://doi.org/10.1016/j.ijhydene.2010.01.027.

Lemmon, E.W., Leachman, J.W., 2008. Revised standardized equation for hydrogen densities for fuel consumption application. J. Res. Natl. Inst. Stand. Technol. 113, 341–350.

Maus, S., Hapke, J., Na Ranong, C., Wüchner, E., Friedlmeier, G., Wenger, D., 2008. Filling procedure for vehicles with compressed hydrogen tanks. Int. J. Hydrog. Energy 33 (17), 4612–4621.

Mintz, M., Elgowainy, A., Gardiner, M., 2009. Rethinking hydrogen fueling: insights from delivery modeling. J. Transp. Res. Board 2139, 46.

Monde, M., Mitsutake, Y., Woodfield, P., Maruyama, S., 2007. Characteristics of heat transfer and temperature rise of hydrogen during rapid hydrogen filling at high pressure. Heat Tran. Asian Res. 36 (1), 13–27.

Nexant Inc., Air Liquide, Argonne National Laboratory, Chevron Technology Venture, Gas Technology Institute, National Renewable Energy Laboratory, Pacific Northwest National Laboratory, TIAX LLC, May 2008. H2A: hydrogen delivery infrastructure analysis models and conventional pathway options analysis results. Report DE-FG36-05GO15032DOE. http://www1.eere.energy.gov/hydrogenandfuelcells/pdfs/nexant_h2a.pdf.

NIST Chemical Webbook: n.d. http://webbook.nist.gov/chemistry/fluid, last consulted December 2017.

Parks, G., Boyd, R., Cornish, J., Remick, R., May 2014. Hydrogen Station Compression, Storage, and Dispensing Technical Status and Costs. NREL Technical Monitor NREL/BK-6A10-58564, https://www.nrel.gov/docs/fy14osti/58564.pdf.

Reddi, K., Elgowainy, A., Sutherland, E., 2014. Hydrogen refueling station compression and storage optimization with tube-trailer deliveries. Int. J. Hydrog. Energy 39, 19169–19181. https://doi.org/10.1016/j.ijhydene.2014.09.099.

Rothuizen, E., Rokni, M., 2014. Optimization of the overall energy consumption in cascade fueling stations for hydrogen vehicles. Int. J. Hydrog. Energy 39, 582–592. https://doi.org/10.1016/j.ijhydene.2013.10.066.

SAE International, July 2014. Surface Vehicle Standard. J2601 Fueling Protocols for Light Duty Gaseous Hydrogen Surface Vehicles. http://www.sae.org/technical/standards/J2601_201407.

Schneider, J., Suckow, T., Lynch, F., Ward, J., Caldwell, M., Tillman, J., Mathison, S., et al., 2005. Optimizing hydrogen vehicle fueling. NHA 2005, http://static1.squarespace.com/static/53ab1feee4b0bef0179a1563/t/543e7eeae4b0983640ec4b93/1413381866875/NHA+2005+-+Optimizing+Hydrogen+Vehicle+Refueling.pdf.

Smith, R. (Ed.), 2005. Chemical Process. John Wiley & Sons, New York, p. 273.

Staffell, I., Green, R., 2013. The cost of domestic fuel cell micro-CHP systems. Imperial College Business Scholl of London, UK. Int. J. Hydrog. Energy 38 (2), 1088–1102. https://doi.org/10.1016/j.ijhydene.2012.10.090.

Wipke, K., Sprik, S., Kurtz, J., Ramsden, T., Ainscough, C., Saur, G., 2012. National Fuel Cell Electric Vehicle Learning Demonstration Final Report. National Renewable Energy Laboratory. http://www.nrel.gov/hydrogen/pdfs/54860.pdf.

Woodfield, P.L., Monde, M., Mitsutake, Y., 2007. Measurement of averaged heat transfer coefficients in high-pressure vessel during charging with hydrogen, nitrogen or argon gas. J. Therm. Sci. Technol 2 (2), 180–191.